Purdue University
Purdue e-Pubs

Department of Electrical and Computer Engineering Technical Reports

Department of Electrical and Computer Engineering

4-1-1989

InSb/CdTe Heterostructures Grown by Molecular Beam Epitaxy

Jack L. Glenn Jr
Purdue University

Sungki O.
Purdue University

Robert L. Gunshor
Purdue University

Leslie A. Kolodziejski
Massachusetts Institute of Technology

Follow this and additional works at: https://docs.lib.purdue.edu/ecetr

Glenn, Jack L. Jr; O., Sungki; Gunshor, Robert L.; and Kolodziejski, Leslie A., "InSb/CdTe Heterostructures Grown by Molecular Beam Epitaxy" (1989). *Department of Electrical and Computer Engineering Technical Reports.* Paper 651.
https://docs.lib.purdue.edu/ecetr/651

This document has been made available through Purdue e-Pubs, a service of the Purdue University Libraries. Please contact epubs@purdue.edu for additional information.

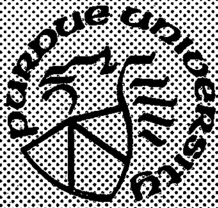

InSb/CdTe Heterostructures Grown by Molecular Beam Epitaxy

Jack L. Glenn, Jr.
Sungki O
Robert L. Gunshor
Leslie A. Kolodziejski*
Masakazu Kobayashi
Nobuo Otsuka
Arto V. Nurmikko**

TR-EE 89-19
April, 1989

School of Electrical Engineering
Purdue University
West Lafayette, Indiana 47907

***Massachusetts Institute of Technology**
****Brown University**

InSb/CdTe HETEROSTRUCTURES GROWN BY MOLECULAR BEAM EPITAXY

Jack L. Glenn, Jr.
Sungki O.
Robert L. Gunshor
Leslie A. Kolodziejski*
Masakazu Kobayashi
Nobuo Otsuka
Arto V. Nurmikko**

School of Electrical Engineering
Purdue University
West Lafayette, IN 47907

TR-EE 89-19
April 1989

* Massachusetts Institute of Technology
** Brown University

TABLE OF CONTENTS

Page

LIST OF TABLES v

LIST OF FIGURES vi

ABSTRACT ix

CHAPTER 1 - INTRODUCTION 1

CHAPTER 2 - PREVIOUS MBE of InSb - CdTe 5

2.1 (100) InSb / (100) InSb Substrates 5
2.1.1 Surface Analysis 5
2.1.2 Crystal Analysis 7
2.1.3 InSb Substrate Preparation 8
2.2 (100) CdTe / (100) InSb Substrates and Epilayers 8
2.2.1 Layer Examination 8
2.2.2 Interfacial Analysis 10
2.3 (100) InSb/CdTe Multilayer Structures 11
2.4 Conclusions 12

CHAPTER 3 - HOMOEPITAXY of (100) InSb / (100) InSb SUBSTRATES 14

3.1 Overview of MBE 14
3.2 Molecular Beam Epitaxy System 14
3.2.1 Equipment 14
3.2.2 Sample Temperature 17
3.2.3 Source Materials 17
3.2.4 Substrate Preparation 19

Page

3.3 (100) InSb Homoepitaxial Layers....................19
3.3.1 Oxide Desorption and Epitaxy....................19
3.3.2 Structural Analysis....................24
3.3.3 Optical Analysis....................28
3.3.4 Non-idealities....................28
3.4 Conclusions....................30

CHAPTER 4 - DUAL CHAMBER HETEROEPITAXY of (100) InSb - CdTe....................31

4.1 (100) CdTe / InSb Single Heterostructures....................31
4.1.1 Transferral of InSb Epilayers....................31
4.1.2 Growth of CdTe/InSb....................32
4.1.3 Structural Analysis....................32
4.1.4 Optical Analysis....................34
4.1.4.1 Photoluminescence....................34
4.1.4.2 Modulated Reflectance....................39
4.2 (100) CdTe / InSb Double Heterostructures....................39
4.2.1 Growth of InSb and CdTe layers....................41
4.2.2 Structural Analysis....................43
4.2.3 Optical Analysis....................43
4.3 Conclusions....................46

CHAPTER 5 - SINGLE CHAMBER HETEROEPITAXY of (100) InSb - CdTe....................47

5.1 Overview....................47
5.2 Setup....................48
5.2.1 Use of Antimony Cracking Furnace....................48
5.2.2 Substrate Preparation....................50
5.3 Continuous Growth of InSb - CdTe Multilayers....................50
5.3.1 Growth Process....................50
5.3.2 Structural Analysis....................51
5.3.3 Optical Analysis....................52

Page

5.4 Interrupted Growth of InSb - CdTe Multilayers 55
5.4.1 Growth Process....................55
5.4.2 Structural Analysis....................57
5.5 Conclusions 59

CHAPTER 6 - SUMMARY AND FUTURE RESEARCH 60

LIST OF REFERENCES 62

APPENDIX A 66

ACKNOWLEDGEMENTS 70

LIST OF TABLES

Table Page

3.1 Elemental and compound source materials for effusion cells 18

3.2 InSb (100) Substrates 20

3.3 Cleaning procedure for molybdenum blocks 21

A.1 Parameters for calculating the indium and antimony flux for a 60cc crucible 69

LIST OF FIGURES

Figure — Page

2.1 RHEED patterns for growth of (100) InSb epilayer on (100) InSb substrate as a function of Sb:In flux ratio and substrate temperature. The narrow region labled "transition region" is characterized by a pseudo-(4x3) RHEED pattern. Reprinted from Oe et al. [20] 6

2.2 InSb/CdTe heterojunction band diagram (reprinted from van Welzenis, et. al. [3]) and possible valence band offset values: 9

3.1 Schematic diagram of Perkin Elmer 430 MBE system. 15

3.2 An AES scan of an InSb substrate at 350 ° C prior to oxide desorption. The surface appears to be nearly free from carbon 23

3.3 $(2\sqrt{2}x\sqrt{2})45°$ RHEED patterns recorded after the growth of a (100) InSb homoepilayer in the (a) [110] and (b) $[\bar{1}10]$ directions 25

3.4 X-ray DCRC (004) trace for a 2μm (100) InSb homoepitaxial layer grown at 330 ° C. 26

3.5 Bright field TEM micrograph showing the (110) face of an InSb epilayer grown on InSb substrate. Dark features at the homointerface may be In oxides, Sb oxides, In or Sb 27

3.6 Photoluminescence spectra of a 2μm (100) InSb epilayer and InSb substrate 29

Figure Page

4.1 RHEED patterns for the growth of (100) CdTe on a (100) InSb epitaxial layer: (a) InSb epilayer [$\bar{1}$10] after transfer to the CdTe chamber, and CdTe layer during growth (t = 35 min) in the (b) [$\bar{1}$10] and (c) [110] directions. 33

4.2 Cross-sectional TEM (200 kV) high resolution electron micrograph of a CdTe/InSb epilayer interface in the [100] projection. 35

4.3 (004) X-ray DCRC trace of a 1.3μm CdTe layer on a 0.5μm InSb homoepitaxial layer. 36

4.4 Low temperature (8K) photoluminescence of a 1.3μm CdTe epilayer grown on an InSb epilayer.
Excitation conditions are (a) power density = 1.68 W/cm^2 and (b) power density = 230 mW/cm^2.
Dominant band-edge feature is free exciton (n=1) at 1.596eV. 37

4.5 Low temperature (8K) photoluminescence of a 1.3μm CdTe epilayer grown on an InSb epilayer (as shown in Figure 4.4).
Near band-edge features at: 1.596 eV (n=1) free exciton, 1.5984 eV (polariton), and 1.6034 eV (n=2) free exciton. 38

4.6 Piezomodulated reflectivity spectrum of a 1.3μm CdTe epilayer grown on an InSb epilayer. Inset: Theoretical fitting to the first derivative of a Lorentzian function.
Reprinted from Lee et al. [42] 40

4.7 RHEED patterns observed during the growth of an InSb (160Å) quantum well structure: (a) t = 5 sec, (b) t = 75 sec, (c) t = 115 sec, and (d) after film growth (t = 152 sec). 42

4.8 Cross-sectional dark field TEM micrograph of CdTe/InSb double heterostructure in the [110] projection.
Dark stripe is the 160Å InSb single quantum well surrounded by the CdTe (light contrast). 44

Figure Page

4.9 Low temperature (10K) infrared luminescence of an InSb active layer (5600Å), in double heterostructure configuration, compared to an InSb substrate. 45

5.1 Schematic diagram of the antimony cracking furnace, supplied by EPI systems. The cracker was used for growth of InSb in the dual III-V/II-VI growth chamber. 49

5.2 Cross sectional TEM micrograph in the [110] direction showing a CdTe/InSb multilayer structure. The structure was grown at 280 ° C with an antimony cracking temperature of 850 ° C. 53

5.3 Cross sectional [110] TEM micrograph showing a CdTe/InSb multilayer structure grown with an antimony cracking temperature of 1040 ° C. Light contrast regions are the 167Å CdTe layers and dark contrast regions are the 163Å InSb layers. 54

5.4 X-ray DCRC scan (004) of a 1μm CdTe epilayer grown on an InSb epilayer at 310 ° C. Scan was taken using a four-pass Si monochromator 56

5.5 X-ray DCRC scan (004) of a 15 period CdTe/InSb multilayer heterostructure grown at a substrate temperature of 310 ° C. Feature "InSb" is attributed to the InSb substrate, feature "0" is attributed to the primary diffraction from the multilayer region and features "$\pm$1 and "$\pm$2" are attributed to diffraction satellites from feature "0". 58

A.1 Indium-flux versus cell-temperature for a 60cc crucible. 67

ABSTRACT

Jack L. Glenn, Jr. M.S, Purdue University. December, 1988. InSb / CdTe Heterostructures Grown by Molecular Beam Epitaxy. Major Professor: Robert L. Gunshor

Given the potential for quantum effect device application, the growth, by molecular beam epitaxy, and characterization of InSb-CdTe heterostructures is described. Two procedures for growth of these heterostructures are employed. For the growth of InSb/CdTe double heterostructures, InSb and CdTe layers are grown in separate MBE growth chambers connected via an ultrahigh vacuum transfer module. Here, antimony originating from a compound InSb source oven is used for growth of InSb layers. For the growth of CdTe/InSb multiple quantum well structures, InSb and CdTe layers are grown in a single MBE growth chamber, where antimony is derived from an antimony cracking furnace.

To study the optical nature of heteroepitaxially grown InSb, infrared photoluminescence from InSb based double heterostructures has been examined. Despite the transferral of grown layers between III-V and II-VI chambers, luminescence gathered from "thick" InSb active layers has shown the existence of recombination features which are similar to bulk InSb. For multilayer structures, grown in a single chamber with the use of an antimony cracker, emphasis has been placed on structural examination by transmission electron microscopy and x-ray diffraction techniques. Examination of multilayer

structures by transmission electron microscopy suggests that the cracker may be useful for the growth of InSb at low substrate temperatures and low growth rates. Using the cracker, CdTe/InSb superlattice structures have been grown showing multiple satellite peaks in the x-ray diffraction spectrum.

CHAPTER I
INTRODUCTION

The creation of thin film heterostructures which exploit reduced dimensionality has given semiconductor research a new direction. Crystal growth by means of molecular beam epitaxy (MBE) is at the forefront of these efforts due to the ultrahigh vacuum environment and atomic level controllability which it provides. To this end, a multiple chamber MBE research facility has been established at Purdue University. Accounting for a large portion of the research to date is an effort to produce high quality InSb-CdTe thin film heterostructures. Motivation for this work stems from the desire to utilize narrow-gap InSb in quantum well configurations with nearly lattice matched ($\delta a/a = 0.05\%$) wide-gap CdTe. Band offset values determined by theoretical and experimental means have indicated that Type 1 carrier confinement should exist in a CdTe-InSb-CdTe quantum well of proper dimensions [1,2]. Uniformly strained single crystal heterostructures and quantum wells may yield tunable infrared detectors spanning the 2 to 5.5 μm range [3]. Single InSb-CdTe heterostructures are also predicted to yield an ultra-high mobility, two dimensional electron gas at the hetero-interface [4]. In the event that very high electron mobilities can be achieved, a high electron mobility transistor (HEMT) structure might be possible.

To date, growth of high quality InSb and CdTe epitaxial layers has been achieved by numerous workers on both InSb [5-9] and CdTe [10] bulk substrates, and InSb epilayers [7,11-13]. Multilayer CdTe/InSb structures have also been grown [11-17]. Problems have been encountered, however, due to a difference in the optimal growth conditions for CdTe on InSb ($T \leq 200\,^\circ C$) [5] and for InSb on CdTe ($225\,^\circ C < T < 275\,^\circ C$) [10]. Electrical properties for InSb layers grown on InSb substrates have been shown to be

optimal for layers grown between 360 °C and 420 °C [9,18]. Mixed interfacial layers composed of In_2Te_3 and segregated antimony have been reported for CdTe layers grown on InSb substrates under stoichiometric conditions at temperatures above 150 °C [19]. The extent of intermixing between InSb and CdTe layers was also reported to increase with an increase in growth temperature as judged by secondary ion mass spectroscopy (SIMS) [8]. Cross doping between III-V and II-VI source materials used in the same MBE chamber has been reported to cause significant incorporation of tellurium in InSb layers grown with a CdTe source present [9].

In light of the aforementioned tendency for InSb and CdTe to auto-dope one another, two MBE chambers have been utilized for the isolated growth of (100) InSb and (100) CdTe epitaxial layers. For growth of InSb layers, polycrystalline InSb and elemental indium source ovens were used in the III-V chamber. CdTe layers were derived from a single compound CdTe source in the II-VI growth chamber. CdTe/InSb/CdTe (100) double heterostructures were fabricated by repeatedly transferring the InSb and CdTe layers through an ultra-high vacuum (mid 10^{-10} Torr) transfer tube to the alternate III-V or II-VI chamber. During the sample transferral process, InSb and CdTe film surfaces were not passivated with any form of protective material.

Given the need to grow heterostructures of more than a few periods in length, InSb-CdTe multilayer structures have been grown in a single MBE chamber. For the creation of a single III-V/II-VI growth chamber, an antimony cracking furnace and indium source oven were installed into the II-VI chamber, previously designated for the growth of CdTe layers. The cracker was primarily chosen to explore the low temperature growth of InSb using Sb_2. As an additional consideration, however, the general design of the cracking cell suggested a level of self-isolation from the in-migration of atomic species, such as tellurium. Using the cracker, multilayer structures, up to 20 periods in length, were grown on CdTe buffer layers to provide a degree of electrical isolation from the (100) InSb or (100) CdTe substrate.

To provide further motivation for the aforementioned crystal growth procedures, chapter 2 will summarize previous MBE research performed on the InSb/CdTe material system. Primary emphasis will be placed on

description of the MBE crystal growth processes which have been employed by previous workers. Epitaxy of InSb on InSb substrates and epitaxy of CdTe on both InSb substrates and InSb epitaxial layers will encompass the majority of the discussion to reflect the amount of work which has been previously performed on these topics. Other points of mention will be InSb substrate preparation methods and the examination of InSb/CdTe interfacial regions by previous workers.

To lay the ground work for the growth of InSb/CdTe heterostructures, chapter 3 will contain a detailed description of the 430 MBE facility and describe the homoepitaxy of (100) InSb epilayers on (100) InSb substrates. The preparation of InSb substrates, the conditioning of source materials, and a description of the nucleation and growth of InSb layers will be described. Use of reflection high energy electron diffraction (RHEED) in determining growth conditions and general film quality will be discussed. Analysis of these films by x-ray double-crystal rocking curves (DCRC), and transmission electron microscopy (TEM) will be presented. Optical analysis by infrared photoluminescence (PL) will be presented to establish the optical properties of these films and to serve as a basis for comparison with heteroepitaxially grown InSb layers.

Chapter 4 will discuss the dual chamber heteroepitaxy of (100) CdTe on (100) InSb epilayers and the growth of (100) CdTe/InSb double heterostructures. Emphasis will be on the growth and characterization of heteroepitaxial CdTe and InSb layers. The structural and optical properties of single CdTe buffer layers, grown on InSb epilayers, will be examined by TEM, DCRC and PL measurement techniques to assess their utility for growth of InSb based heterostructures. The growth, by substrate transferral, of InSb active layers (160Å - 5600Å) on CdTe buffer layers, followed by the growth of CdTe capping layers (2200Å), will be described. Double heterostructures (CdTe/InSb/CdTe) grown in this way will be examined by TEM and Raman scattering in an attempt to determine interfacial and in-layer structural properties. The InSb active layer will be examined by PL and comparisons will be made with InSb epilayers and bulk material.

Chapter 5 will describe the growth and characterization of CdTe/InSb multiple quantum well and superlattice structures grown in a single MBE chamber. Primary emphasis will be on describing of the use of the antimony cracking furnace for growth of InSb at low substrate temperatures (280 to 310 ° C) and very low growth rates (0.2 - 0.4 Å/second). CdTe substrate preparation techniques will be outlined along with procedures for the nucleation and growth of homoepitaxial CdTe layers. Examination of layer quality and interfacial nature of multiple quantum well structures by TEM and DCRC measurements will be presented.

A summary of research and a discussion of conclusions will be given in chapter 6. Ideas for future research projects will be presented in attempting to extend the efforts began here. Appendix A, presented after chapter 6, will detail the procedure used in formulating the effusion cell flux-vs-temperature curves for the indium and antimony ovens.

CHAPTER 2
PREVIOUS MBE of InSb - CdTe

A large amount of research has been performed on the MBE growth of single InSb layers on CdTe and on the growth of single CdTe layers on InSb. A review of this work was helpful in guiding our research efforts. The following section will thus be dedicated to this topic. Primary emphasis will be given to previous work performed on the MBE growth of these semiconductors and relevant examination of material properties.

2.1 (100) InSb / (100) InSb Substrates

2.1.1 Surface Analysis

Thin InSb films of (100) orientation have been grown by MBE on InSb substrates by a number of groups [7,8,20,21]. Oe et al. [20] and Noreika et al. [21] have identified detailed RHEED reconstruction features which were dependent upon substrate temperature and flux ratio (J_{Sb}/J_{In}), and are summarized in Figure 2.1. Noreika et al. [21] report that two phase growth, consisting of poly-crystalline InSb and hexagonal phase antimony, resulted when layers were grown with a substrate temperature below approximately 250° C. Growth under an excess of indium flux ($J_{Sb}/J_{In} < 1$) was reported to result in a c(8x2) RHEED reconstruction [20,21], Excess antimony flux was reported to yield a wide range of surface reconstruction features strongly dependent upon the exact flux ratio and substrate temperature [20,21]. A unity flux ratio was seen to give a "psuedo"-(4x3) pattern, where the three-fold surface reconstruction was seen to be unevenly spaced between the bulk features [10,20,21]. In nearly every case, the InSb films were derived from elemental antimony and indium sources which yield predominantly Sb_4 and In_1 species.

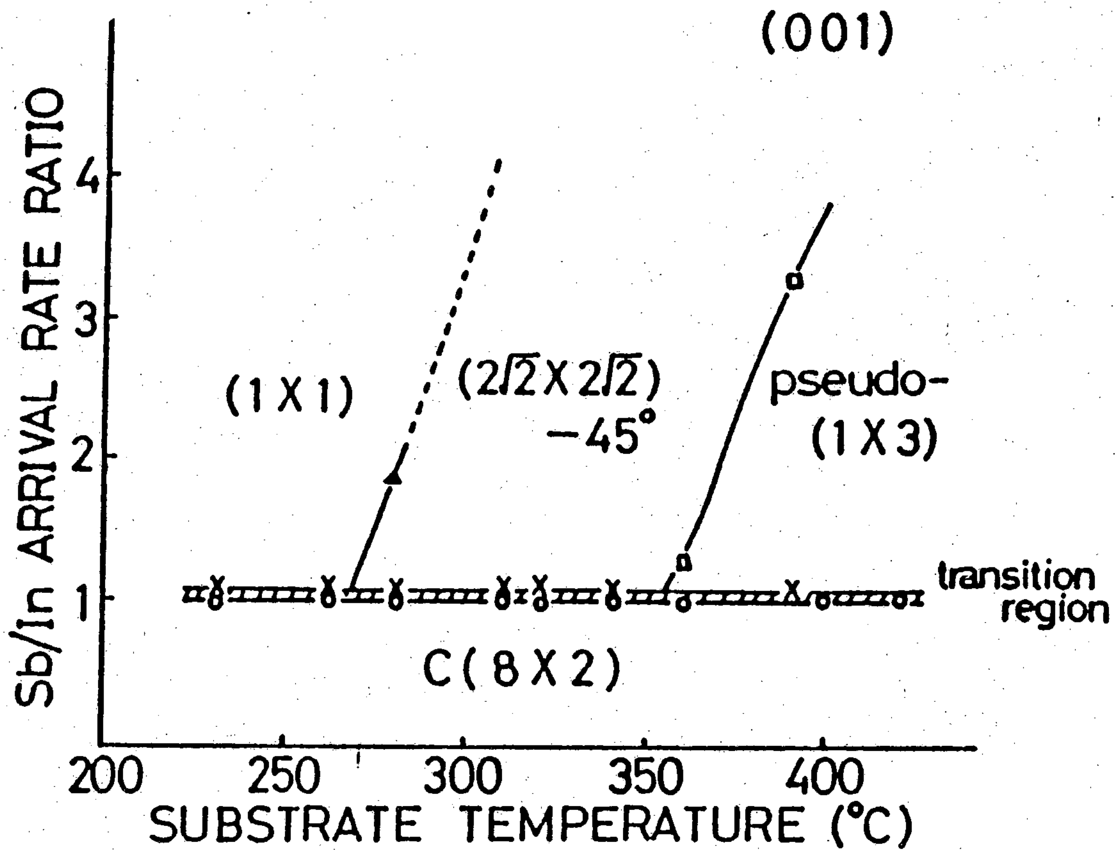

Figure 2.1
RHEED patterns for growth of (100) InSb epilayer on (100) InSb substrate as a function of Sb:In flux ratio and substrate temperature. Reprinted from Oe et al. [20].

2.1.2 Crystal Analysis

Reports of structural data by TEM have shown that crystalline InSb layers can be grown on InSb substrates over a range of growth conditions ($230\,^{\circ}C < T < 510\,^{\circ}C$), despite the presence of indium precipitates at the film/substrate interface [7,8]. These precipitates, which were reported to be induced by *in-situ* surface preparation (ion bombardment followed by thermal annealing or thermal oxide desorption under an Sb_4 flux), were shown to be aligned with the InSb matrix and are therefore coherent with the interface. Films grown below $230\,^{\circ}C$ were reported by TEM to be polycrystalline regardless of the flux condition used. The poor quality of InSb layers grown at low temperatures has been attributed to a reduction in the mobility of molecular species which are adsorbed onto the InSb surface prior to being incorporated into the lattice [8] The aforementioned InSb layers were grown with the use of an elemental antimony source yielding the tetrameric Sb_4 species.

Transport measurements have been reported on InSb films and bulk material [9,18,22,23]. Experiments by Williams et al. [9], have indicated that unintentional n-type carrier concentrations are lowest for InSb layers grown at $420\,^{\circ}C$ and $J_{Sb}/J_{In} = 1.4$. It was also reported [9] that the incorporation of tellurium, an n-type dopant, into the grown InSb films was limiting the reduction in carrier concentration. Furthermore, the tellurium doping was reported to be derived from the antimony source which was used for growth of InSb films. Tellurium atoms from a compound CdTe source, used in the same MBE growth chamber as the antimony source, were reported to be the cause of contamination in the antimony source material [9]. The contamination of antimony source material with tellurium was further reported to occur as a result of merely loading antimony and CdTe sources in the same chamber, with or without baking the system. Problems with the growth of multilayer CdTe/InSb structures in a single chamber with optimal carrier transport properties in the InSb layer would not be unexpected.

2.1.3 InSb Substrate Preparation

Several methods for InSb substrate preparation have been reported. Typically, InSb substrates were degreased in liquid solvents followed by etching in an acid solution such as 25:4:1 (lactic acid:HNO_3:HF) [21] or 10:1 (lactic acid:HNO_3) [24]. The substrates were then rinsed in deionized water and dried in nitrogen gas (N_2). InSb wafers were commonly mounted using a metal such as indium [15,24] or gallium [23]. In some cases, metal films (especially indium) were avoided due to reports of preferential diffusion into substrates during growth and the suspected formation of high temperature indium-molybdenum alloys [21,23]. An alternative to bonding the substrate with the use of a metal film was reported to be the use a solution of graphite in water (aqua-dag). Reports also differ as to the optimal method for removing InSb surface oxides (*in-situ*) prior to film growth. Thermal desorption of the oxide layer has been reportedly achieved by heating samples to temperatures above 400 ° C with the use of an Sb_4 flux [11,13]. Alternately, several workers have preferred to use repeated cycles of argon ion bombardment followed by thermal annealing to remove native oxides [7,8]. Several authors [9,20,21,25] have reported the existence of a c(8x2) indium-stabilized surface in the RHEED pattern, after oxide removal.

2.2 (100) CdTe / (100) InSb Substrates and Epilayers

2.2.1 Layer Examination

In addition to the efforts aimed at optimizing InSb epilayer growth, a great deal of work has been previously reported on the growth and characterization of (100) CdTe films on (100) InSb substrates [5-9] and InSb epilayers [7]. Figure 2.2 shows a hypothetical band diagram for a CdTe/InSb heterojunction [3]. Several valance band offset values which have been proposed by theoretical and experimental means are listed in the figure caption [1,2,26]. For growth of CdTe layers, primary emphasis has been reportedly placed on InSb substrate preparation by argon ion bombardment and thermal annealing procedures. Photoluminescence (PL) studies have been reported indicating that the best optical characteristics, specifically, dominant free exciton and bound exciton transitions, will occur in films grown between

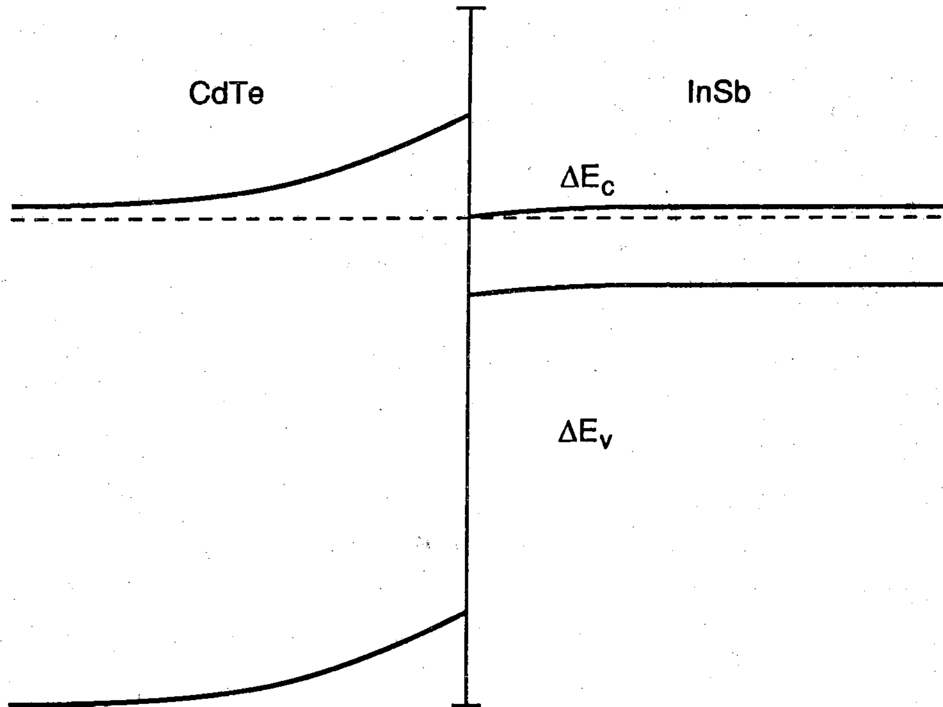

Figure 2.2 InSb/CdTe heterojunction band diagram (reprinted from van Welzenis, et. al. [3]) and possible valence band offset values:

ΔE_v(eV)	METHOD	REFERENCE
0.96	electron affinity rule	Anderson [26]
0.84	tight binding model	Tersoff [1]
0.87	soft-XPS	Mackey et. al. [2]

160 °C and 200 °C [5]. These results have been confirmed by structural data gathered on CdTe films grown at 200 °C. In this case, diffraction peaks, generated by the DCRC technique, have been reported with full width at half maximum (FWHM) values of less than 20 arc seconds for the best CdTe layers [5]. All of the aforementioned work was performed at growth rates between 1 and 2 Å/second. With the exception of very recent work by Golding et al. [13], CdTe films have been previously grown using a compound CdTe source known to yield congruent amounts of 2Cd and Te_2 species at cell temperatures of interest [6,25]. In addition, Farrow et al. [26] have utilized an insert to restrict the molecular beam emanating from the CdTe source oven to a 3mm diameter hole.

2.2.2 Interfacial Analysis

Despite evidence for high quality CdTe layers grown at 200 °C, TEM analysis has indicated that the sharpest heterointerfaces occur for layers grown on InSb at 150 °C. Unfortunately, CdTe is observed to be polycrystalline when grown at or below 150 °C. Closer examination of the CdTe/InSb interface has further indicated several problems. A series of studies were undertaken by Mackey et al. [19] in an attempt to examine this interface. Ion cleaned (100) InSb substrates were used for the growth of ultra thin (up to 40 Å) CdTe epilayers at temperatures between 200 °C and 220 °C. Soft x-ray photoelectron spectroscopy (SXPS) and Raman scattering were used to show that the grown CdTe layers possessed large fractions of segregated antimony and In-Te complexes. These complexes were reportedly identified as extra peaks in the Raman scattering data (other than the CdTe LO phonon at 168 cm^{-1}) in the range of 120 and $175 cm^{-1}$. To identify the exact composition of these layers, bulk In_2Te_3 crystals were grown by the horizontal Bridgman method and examined by Raman spectroscopy. While the spacing between the LO phonon peaks in question was the same for both the grown film and bulk sample, a distinct energy shift was seen between peaks characteristic of bulk In_2Te_3 and those characteristic of the film. This was explained [19] by assuming that the lattice mismatch ($\delta a/a = 5\%$) between In_2Te_3 and InSb was elastically accommodated in the grown layer and would therefore produce

a strain shift.

In addition to the studies on (100) InSb substrates, CdTe films were deposited on in-vacuo cleaved (110) InSb surfaces at 250 ° C. Raman scattering and SXPS performed on these films revealed the same In-Te compound formation as for the (100) depositions. In contrast to the (100) surface, which has a slight polar nature with the presence of an indium-stabilized surface, the (110) is completely non-polar and has a stoichiometric surface. Mackey et al. [19] therefore suggest that a preponderance of indium on the nucleating (100) surface is not a prerequisite for the formation of In-Te mixing layers, given that the same formations are observed on the (110) surface. Less emphasis has been paid to the microstructural examination of heterointerfaces formed by the growth of CdTe layers on InSb epitaxial layers. In a related material system, the MBE growth of ZnSe (II-VI) on GaAs (III-V) has been reported in some instances to produce a (Ga,Se) (III-VI) mixing layer at the III-V/II-VI heterointerface [29]. With this fact, it seems clear that the area of interfacial chemistry needs a great deal of exploration as it pertains to III-VI and II-V bonding configurations.

2.3 InSb/CdTe Multilayer Structures

In light of the information presented here, there would seem to be a number of problems associated with InSb/CdTe multilayer growth. First, the previously reported [10] window for growth of InSb on CdTe (225 to 275 ° C) appears to be somewhat incompatible to that for growth of CdTe on InSb (160 - 220 ° C). Further, transport properties for InSb layers indicate the need for growth temperatures in excess of 400 ° C [9,18]. In addition, interfacial regions are reported to form between the respective compound material systems and are reported to increase in thickness as growth temperatures increase. Despite these difficulties, both, our research group [12,14-16], and Golding et al. [13] have very recently reported the growth of multilayer CdTe/InSb structures at temperatures near 300 ° C. A complete discussion of all work on multilayered structures will be addressed in chapter 5.

Reports concerning the heteroepitaxy of InSb on CdTe substrates have been given, but with limited success [10]. In general, the growth of InSb

layers on CdTe appears to be more difficult than the converse, as CdTe substrates are prone to the existence of low angle grain boundaries and other defect related problems. By comparison, InSb substrates are available with very high crystalline quality. An additional tradeoff between InSb and CdTe substrates occurs in the form of substrate resistivities which are currently available. InSb wafers are presently available with maximum resistivities of 1000 ohm-cm [30], in contrast to CdTe wafers which are available with resistivities of 1 Mohm-cm [31]. To this end, the choice between InSb and CdTe substrates presently constitutes a tradeoff between higher structural and higher insulating properties, respectively.

2.4 Conclusions

To summarize this section, the contributions of other workers on the MBE growth and characterization of InSb, CdTe, and InSb/CdTe structures have been reviewed. It was seen that the growth of InSb/CdTe heterostructures has been complicated by a number of difficult problems. For the successful growth of InSb layers with desirable transport characteristics a way must be found to prevent the incorporation of tellurium into the grown InSb layers. One possibility might be to isolate the InSb and CdTe source materials to separate growth chambers. The growth of multilayers would then have to be achieved by some form of sample transferral process between growth chambers. In this case, the question of contaminating the grown InSb or CdTe layer surface would be of primary importance. Alternately, InSb and CdTe layers might be grown in a single chamber, if contamination of the antimony source material, by tellurium, could be minimized. A two-stage furnace or cracking cell might be useful in providing a thermal barrier to the migration of tellurium into the oven, by keeping the oven (especially the cracking end) at elevated temperatures.

The problem of the growth temperature incompatibility between InSb and CdTe epitaxial layers may be difficult to solve. The continuous growth of CdTe and InSb layers becomes a question of whether to raise the CdTe growth temperature or lower that of InSb. To accommodate the problem of interfacial mixing it would appear as though the InSb layer should be grown

at as low a substrate temperature as possible. To achieve this, reports concerning the low temperature growth of GaAs may prove insightful. The low temperature growth of GaAs epilayers has proven more successful when performed at very low growth rates and with As_2 rather than with As_4 [32,33]. Specifically, the density of deep level electronic traps has been shown to decrease for films grown at low temperatures if the films are grown at low growth rates and with As_2. in films grown at low growth rates and low substrate temperatures with dimeric As_2 as compared to those grown with the tetrameric As_4 (under otherwise similar conditions). A possible explanation for the aforementioned reduction in deep level traps (advanced by [32] and [33]) is that the easier surface incorporation of As_2 over that of As_4 may lead to a reduction in arsenic vacancies within the grown layer. In light of these findings, the use of Sb_2 rather than the more conventional Sb_4 species in the low temperature growth of InSb seems an interesting prospect.

CHAPTER 3
HOMOEPITAXY of (100) InSb / (100) InSb SUBSTRATES

3.1 Overview of MBE

A detailed description of the science and technology of molecular beam epitaxy is available in other references [34]. Briefly, MBE is a non-equilibrium crystal growth process performed under ultra high vacuum conditions. Unlike processes for growing bulk material, thin film crystals are grown by the surface migration and kinetic motion of atomic and molecular species, derived from effusion cell furnaces. Control over growth parameters is therefore given to the operator by selection of beam type, beam molecular density and substrate temperature. To the extent that they are physically realizable, a wide variety of thin film semiconductors may be grown, including various metastable structures not available by equilibrium growth techniques, on a wide variety of substrate materials. The success of quantum wells, superlattices and other structures which exploit reduced dimensionality is contingent on the use of exacting crystal growth techniques like MBE.

3.2 Molecular Beam Epitaxy System

3.2.1 Equipment

A diagram of the model 430 Perkin-Elmer MBE system is given in Figure 3.1. In this configuration, three vacuum chambers are used for the growth of III-V and II-VI semiconductors, while a fourth is designated for the deposition of metal films. These chambers are maintained at base pressures in the mid 10^{-11} Torr range using cryogenic, ionic and titanium sublimation pumps. A fifth chamber equipped with Auger electron spectroscopy (AES) capabilities maintains a pressure of $2x10^{-10}$ Torr using an ion pump. Samples may be loaded into the system by either of two cryo-pumped introduction chambers

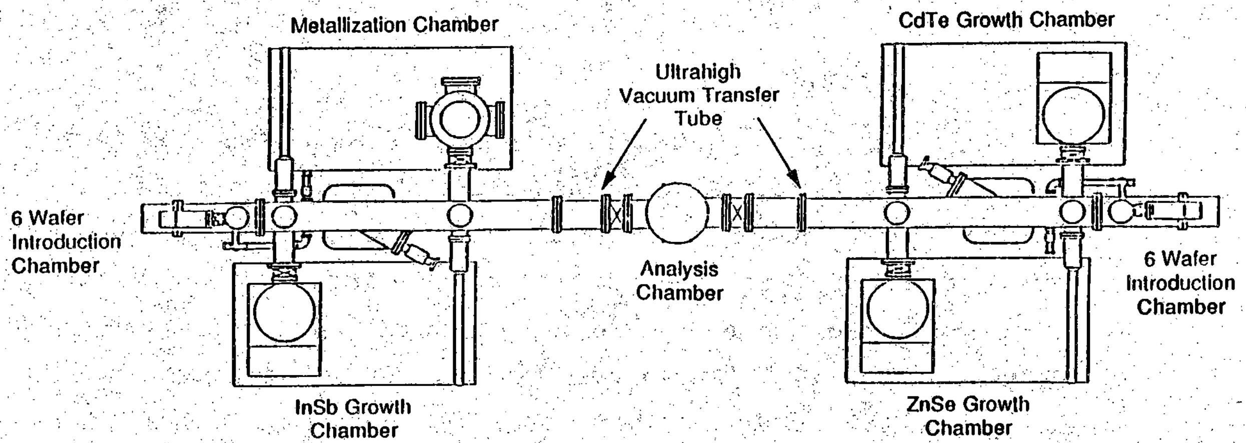

Figure 3.1. Schematic diagram of the Perkin Elmer 430 MBE system.

which can support up to six - 3 inch molybdenum sample holders in a cassette type rack. The cryogenic pump maintains a low 10^{-8} Torr vacuum in the introduction chambers. Interconnecting all of these chambers are two ion pumped transfer tubes which operate in the low 10^{-10} Torr range. A series of trolley mounted forks and probe arms allow for sample manipulation to all points in the system. The addition of new chambers and transfer tubes may take place in a modular fashion allowing for future expansion of the MBE system.

To accommodate a variety of source materials, each growth chamber is equipped with eight source ovens positioned symmetrically in front of a sample manipulator assembly. InSb layers are grown in an "InSb" or "III-V" chamber by use of 60cc effusion cells containing polycrystalline InSb and elemental indium, while for isolation of dopant species, cadmium and tellurium species are restricted to the "CdTe" or "II-VI" chamber in the form of a single 60cc compound CdTe source. It will be pointed out later (chapter 5) that for experiments involving the growth of InSb/CdTe multiple quantum wells, an antimony cracking furnace and elemental indium source oven are placed in the CdTe chamber. All oven crucibles (with the exception of the antimony cracker) are made of pyrolytic boron nitride (PBN). In addition, the CdTe source contains a PBN insert to restrict the flux beam to a 1/8 inch hole. Each chamber is separated from the transfer tubes by an UHV gate valve to allow independent servicing and proper isolation of cross doping material systems.

In order to monitor *in-situ* conditions, a variety of analytical equipment has been installed in each growth chamber. A measure of residual or background pressure is given by a nude ion gauge located in the ion pump well. A second gauge located behind the sample manipulator assembly is used to give an indirect measure of beam flux. More accurate readings of oven flux are obtained by measuring the frequency changes in a quartz crystal oscillator which may be placed near the actual substrate position. The presence of residual atomic or moleculer species may be determined by a quadrupole mass analyzer (QMA) located near the cryopump. A 10 kVolt reflected high energy electron diffraction (RHEED) apparatus, and adjacent phosphorus screen are

used for the study of film growth processes, and as an indicator of film quality. Images projected onto the RHEED screen represent a Fourier transform of the substrate surface and as such provide information on reciprocal lattice periodicity.

3.2.2 Sample Temperature

Sample temperature is measured by a non-contact thermocouple positioned in the center of each sample heater assembly. The 3 inch sample blocks used in this work are disc shaped and hollow in the center. Once loaded onto the growth manipulator assembly, the sample block covers the heater and thermocouple, creating a closed cavity. The cavity radiation is then read by the thermocouple as the block temperature. Optionally, an infrared pyrometer may be used to measure the substrate/film temperature through a sapphire window in the source flange [35]. This was deemed necessary in some cases where the thermocouple reading was found to deviate from block to block. The pyrometer works by measuring the black body radiation emanating from the material it is focussed onto. Since the material will not be a perfect emitter of radiation, the pyrometer will accept input for the actual emissivity of the object and will correct the output temperature accordingly. Block temperatures have also been calibrated by observing the phase change of a Au:Ge eutectic at 356 °C. The eutectic consists of a 500Å thick gold film evaporated onto an etched, degreased germanium substrate. At 356 °C, the Au:Ge interface changes as the two materials form an alloy. The result is a reduction in surface specularity. Taken together, the different temperature calibration techniques allow for redundancy in determining the actual block temperature.

3.2.3 Source Materials

Source materials for the growth of InSb and CdTe layers may be purchased from many vendors. Table 3.1 summarizes pertinent information about the purity and origin of source materials. After the loading of source materials, and the subsequent system bakeout, each oven was outgassed for 4 hours at elevated temperatures to drive off surface oxides and residual

Table 3.1. Elemental and compound source materials for effusion cells.

MATERIAL	FORM	PURITY	VENDOR
Indium	1mm bead	6N	Johnson Matthey AESAR
Antimony	random lump	6N5	Johnson Matthey AESAR
InSb	polycrystalline	6N	Cominco Electronic Materials
CdTe	polycrystalline	5N6+ [36]	II - VI Company Inc.

impurities. To gain a relation between source temperature and molecular beam flux, crystal monitor readings for each oven were taken at various temperatures and plotted against an ideal (Knudsen) curve [34]. As a further measure, indium, antimony, and InSb source materials were separately deposited on etched silicon substrates at room temperature. To give a thickness reading, each silicon substrate was partially shielded from the flux by a piece of nickel foil. An Alpha-step 200 surface profiler was then used to determine the film thickness by scanning across the film-substrate step which was created. By a knowledge of the density of antimony, indium, and InSb in amorphous form a flux could be determined as in Appendix A.

3.2.4 Substrate Preparation

InSb (100) substrates were purchased from Cominco Electronic Materials Inc. in the four types listed in table 3.2. Surface preparation [24] was performed by degreasing the wafer in two cycles of mildly boiling TCA, followed by ultra-sonic cleaning in acetone and methanol. Wafers were then rinsed in de-ionized water and blown dry using nitrogen (N_2) gas. Etching in a solution of 10:1 (lactic acid:HNO_3) was then performed for a period of 90 seconds to remove approximately 1 μm of material. Etching was halted by flooding the etchent solution with de-ionized water, followed by rinsing for several minutes. Samples were then blown dry in N_2 gas and mounted on molybdenum blocks with a very thin film of indium. Cleaning procedure for the Mo blocks used in mounting InSb (and CdTe) substrates is described in table 3.3. For the purpose of temperature calibration in the chamber, a 6 mm square Au:Ge eutectic sample was mounted (with indium) adjacent to each InSb wafer. After mounting the eutectic and InSb substrate, sample holders were placed in the introduction chamber and baked for one hour at approximately 200 °C to drive off water vapor.

3.3 (100) InSb Homoepitaxial Layers

3.3.1 Oxide Desorption and Epitaxy

After loading the InSb substrate into the InSb chamber, the observation of the eutectic change was performed with the sources below measurable flux

Table 3.2 InSb (100) Substrates.

TYPE	DOPANT	$N_{D,A}$ (cm^{-3})	ρ (Ω-cm)
N	tellurium	1.4 - 1.9x10^{17}	7.0 - 7.4x10^{-4}
P	cadmium	3.0 - 4.2x10^{14}	1.5 - 2.5
P	cadmium	1.2 - 1.9x10^{13}	45 - 75
P	cadmium	$\sim$ 2.0x10^{12}	800 - 850

Table 3.3 Cleaning procedure for molybdenum blocks

PROCESS	CHEMICAL	TOOLS	TIME
remove indium		razor blade	
etch indium	HCl	blk holder	1-3 min
rinse	H_2O	blk holder, tongs	5-10 min
etch Mo block	$4H_2O$:$1HNO_3$	blk holder	1-4 min
rinse	H_2O	blk holder, tongs	5 min
etch Mo oxide	HCl	blk holder, tongs	5 min
RINSE:			
acid bkr	H_2O	blk holder, tongs	10 min
degrease bkr	H_2O	blk holder, tongs	30 min
DEGREASE:			
boil	TCA	deg bkr, tongs	5 min
boil	TCA	deg bkr, tongs	5 min
USC	ACE	deg bkr, tongs	5 min
USC	Meth	deg bkr, tongs	5 min
dry	N_2	deg bkr, tongs	

levels. The procedure involved bringing the substrate temperature to a point below 356 °C (typically 300 °C) and raising the temperature by 1 °C/minute thereafter. Upon calibration of the thermocouple temperature, the sample temperature would be lowered to 250 °C and the growth manipulator assembly would be retracted into a down position to shield the substrate from the source ovens. At this point, the indium, antimony and InSb source ovens would be brought up to the desired flux condition, for growth, and allowed to stabilize for one hour. Beam fluxes were next checked by use of the quartz crystal monitor and adjusted if necessary. (Preferential depletion of antimony from the InSb source required use of higher InSb cell temperatures during each successive growth cycle.) After achieving proper beam fluxes, oven shutters were closed and the sample was brought up into the RHEED/growth position at 380 ° C. A faint set of substrate features were sometimes visible in the otherwise diffuse (amorphous oxide) RHEED pattern. When raising the substrate temperature, the diffuse background in the RHEED pattern was seen to gradually decrease in intensity as the oxide layer would begin to desorb. Upon observation of integral order features, and sometimes very faint surface reconstruction features, an elemental antimony source Sb_4 would be opened to replenish preferentially desorbed surface antimony [23].

Full desorption of the oxide layer was characterized by the observation of integral-order and fractional-order (surface reconstruction) streaks in the <110> RHEED patterns. The surface reconstruction present after oxide desorption was not absolutely clear in the RHEED patterns observed. The oxide desorption process was seen to take place through a range of substrate temperatures (430 - 470 ° C). The observation of a wide temperature range, through which the native indium and antimony oxides could desorb, was confirmed by desorption of an oxide layer in the Auger analytical chamber. In this experiment, the surface species on the InSb wafer were monitored by AES during the oxide desorption process. An AES scan for the surface of an InSb substrate prior to oxide desorption is shown in Figure 3.2. For this scan, the surface appears to have large fractions of In, Sb and oxygen, while having almost no registration of carbon. After complete oxide desorption had been observed, the substrate temperature was immediately dropped and the Sb_4

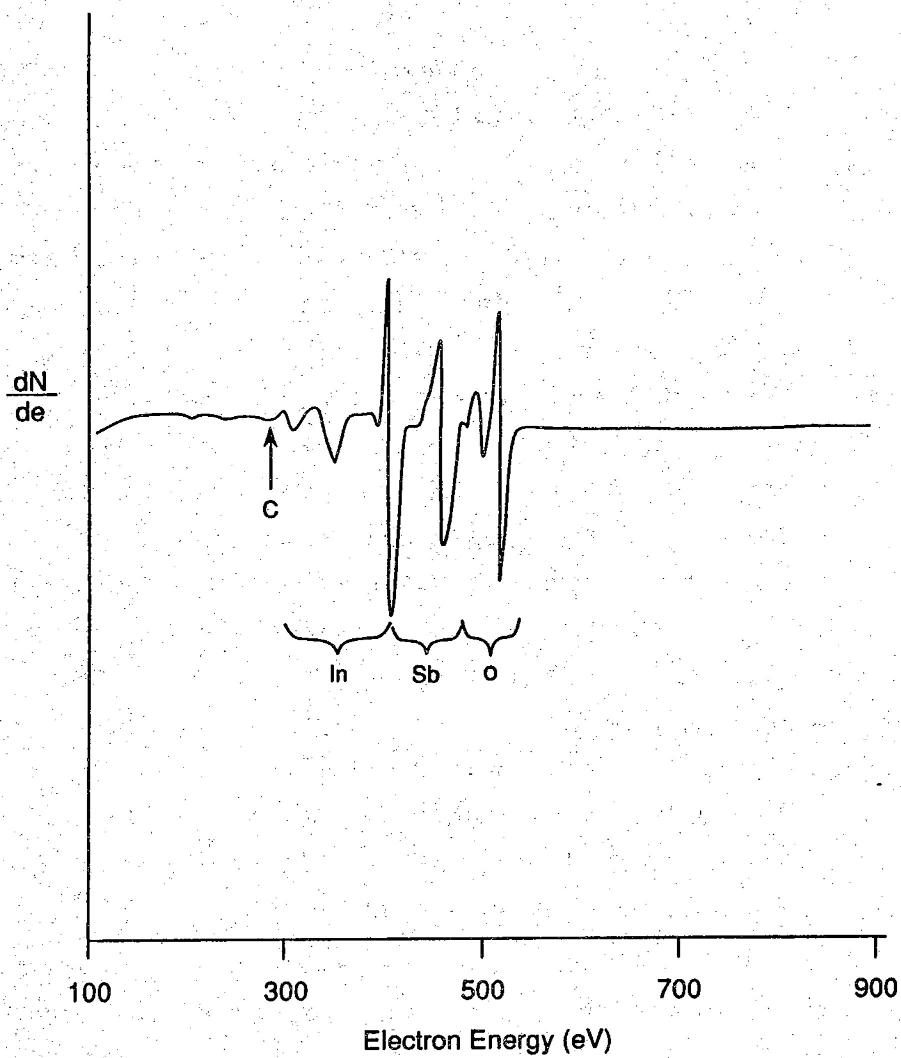

Figure 3.2 An AES scan of an InSb substrate at 350 °C prior to oxide desorption. The surface appears to be nearly free from carbon.

flux discontinued. InSb epilayers were nucleated, by opening the InSb and indium ovens, at a thermocouple reading of 25 °C above the desired growth temperature. During growth of the InSb layer, a $(2\sqrt{2} \times 2\sqrt{2})45°$ surface reconstruction was usually observed after several minutes of film growth. Typical RHEED patterns taken after the growth of an InSb homoepilayer are shown in figure 3.3. InSb layers of up to 2 μm in thickness were grown with the $(2\sqrt{2} \times 2\sqrt{2})45°$ RHEED pattern using a growth rate of 1.2 Å/second.

3.3.2 Structural Analysis

Structural analysis has been performed on InSb layers by DCRC and TEM techniques. DCRC traces have been taken on a 2μm InSb layer in the (004) direction using Cu Kα radiation and 1x1 mm slit sizes. For this purpose, an InSb substrate was utilized as a monochromating crystal (crystal #1). Experiments on a similar InSb substrate were performed to determine the limit of resolution for this set-up. Typical FWHM values for the substrate as a test crystal were 13 arc seconds with values as low as 12 arc seconds being seen infrequently. Diffraction peaks from grown films were typically symmetric in nature and FWHM values of 13 arc seconds were common as shown in Figure 3.4. Transmission electron microscopy (TEM) studies were performed in the Materials Engineering department of Purdue University by D. Li and J. M. Gonsalves under the direction of Dr. N. Otsuka. A bright field TEM micrograph revealing the InSb layer/substrate homointerface is shown in Figure 3.5. Layers were seen to be in intimate contact with the substrate despite the existence of dot-like features at or near the homointerface. These dot-like features are suggestive of precipitate formation, the nature of which is unknown. Previous reports [7,8] speculate that these could be indium droplets. An observation of the spacing between lattice fringes in the TEM image indicates that these precipitates might be In oxides, Sb oxides, In or Sb. As with the previous studies, the quality of InSb layers is apparently uneffected by the existence of these precipitates as they form coherent regions which do not tend to nucleate dislocations or other extended defects.

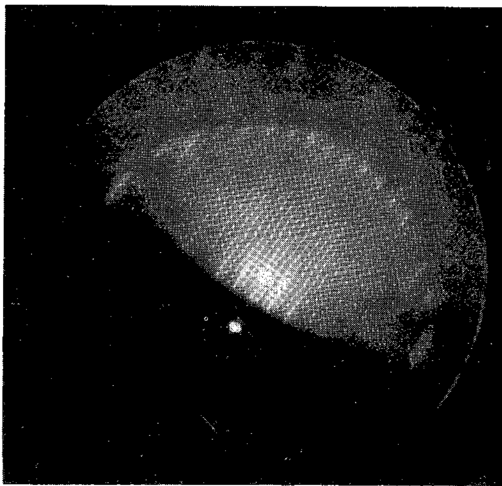

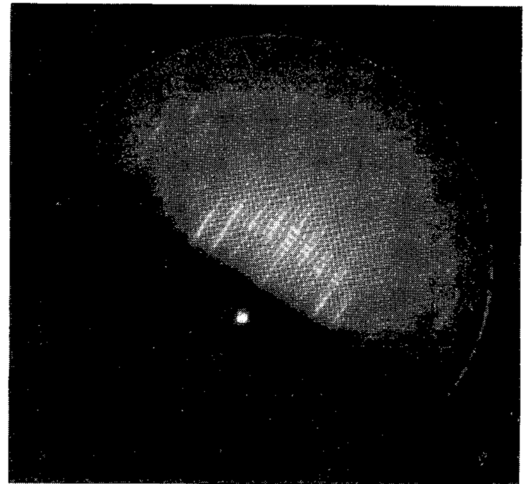

(a) (b)

Figure 3.3 $(2\sqrt{2} \times 2\sqrt{2})45^\circ$ RHEED patterns recorded after growth of a (100) InSb homoepilayer in the (a) [110] and (b) $[\bar{1}10]$ directions.

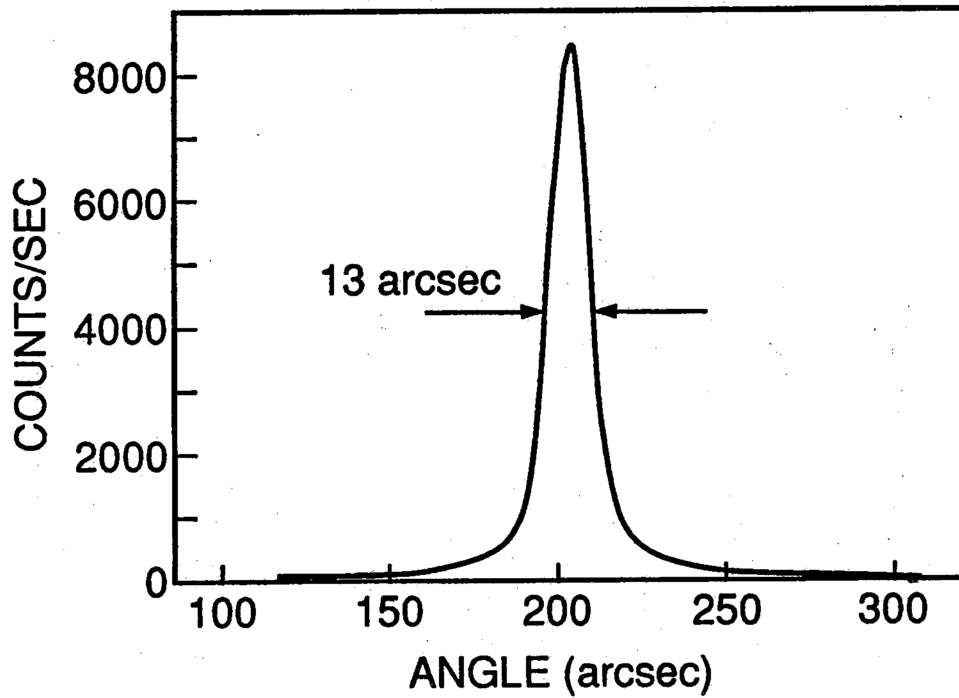

Figure 3.4 X-ray DCRC (004) trace for a 2μm (100) InSb homoepitaxial layer grown at 330 ° C.

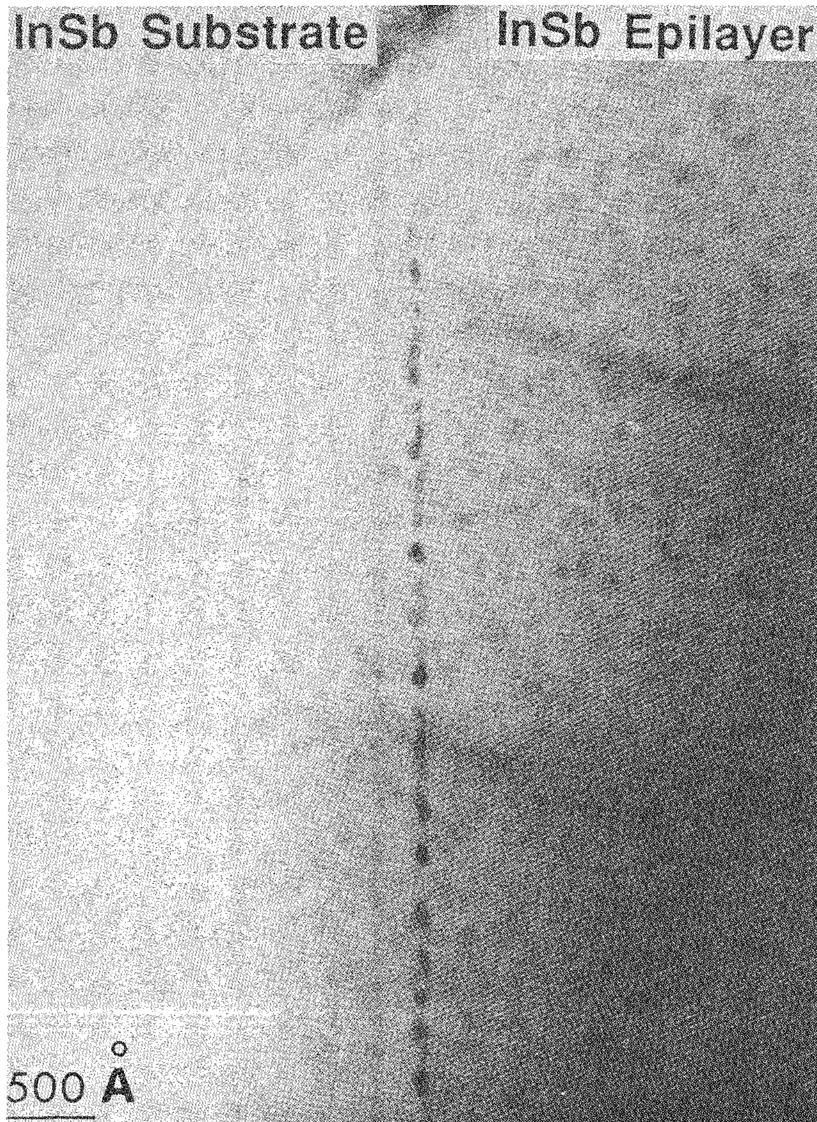

Figure 3.5. Bright field TEM micrograph showing the (110) face of an InSb epilayer grown on InSb substrate. Dark features at the homointerface may be In oxides, Sb oxides, In or Sb.

3.3.3 Optical Studies

Infrared photoluminescence (PL) evaluations of the InSb homoepitaxial layers have been performed at Brown University by M. Haggerott under the direction of Dr. A. V. Nurmikko. For the photoluminescence experiments, InSb samples were excited using YAG and green laser radiation at an incident power of 200mW. Laser light was focussed down to a spot of 500μm in diameter, and luminescence from the InSb samples was collected in a cooled (77K) InSb detector. Figure 3.6. shows PL from an InSb substrate and 2 μm InSb epilayer performed at 10K under identical conditions. Dominant band-to-band recombination is seen for this and other InSb samples, (resembling luminescence from high quality bulk material [37]) appearing at approximately 234 meV. Secondary features are also observed in the range of 228 meV. The origin of the secondary peak in the InSb substrate would appear to be caused by a cadmium acceptor as the substrate is cadmium doped to a level of N_D = 3.0 - 4.2x10^{14} (cm^{-3}). The band-to-band recombination feature observed for the InSb epitaxial layer, is seen to be more intense than for the InSb substrate by a factor of approximately seven. Due to the strong absorption of YAG laser lines in InSb, it is believed that the lower energy feature in the epilayer spectrum (which has been attributed to an impurity related feature) originates from the epilayer itself. Zinc is a possible candidate for the low-intensity feature in the epilayer appearing at 228 meV in high quality InSb bulk material [38]. The presence of zinc in a separate MBE growth chamber (connected by UHV transfer tubes) used for growth of ZnSe or in the indium or antimony source materials might explain the occurrence of a zinc-related recombination feature in the InSb photoluminescence.

3.3.4 Non-idealities

For the majority of InSb films which have been grown at substrate temperatures in the range of 300 to 330 ° C, an unusual phenomenon has been observed in the RHEED patterns during growth. Quite often, the RHEED pattern would be seen to fade in intensity after approximately one hour of growth leaving diminished integral order streaks on the screen. A very sharp $(2\sqrt{2} \times 2\sqrt{2})45°$ reconstructed RHEED pattern could be recovered by

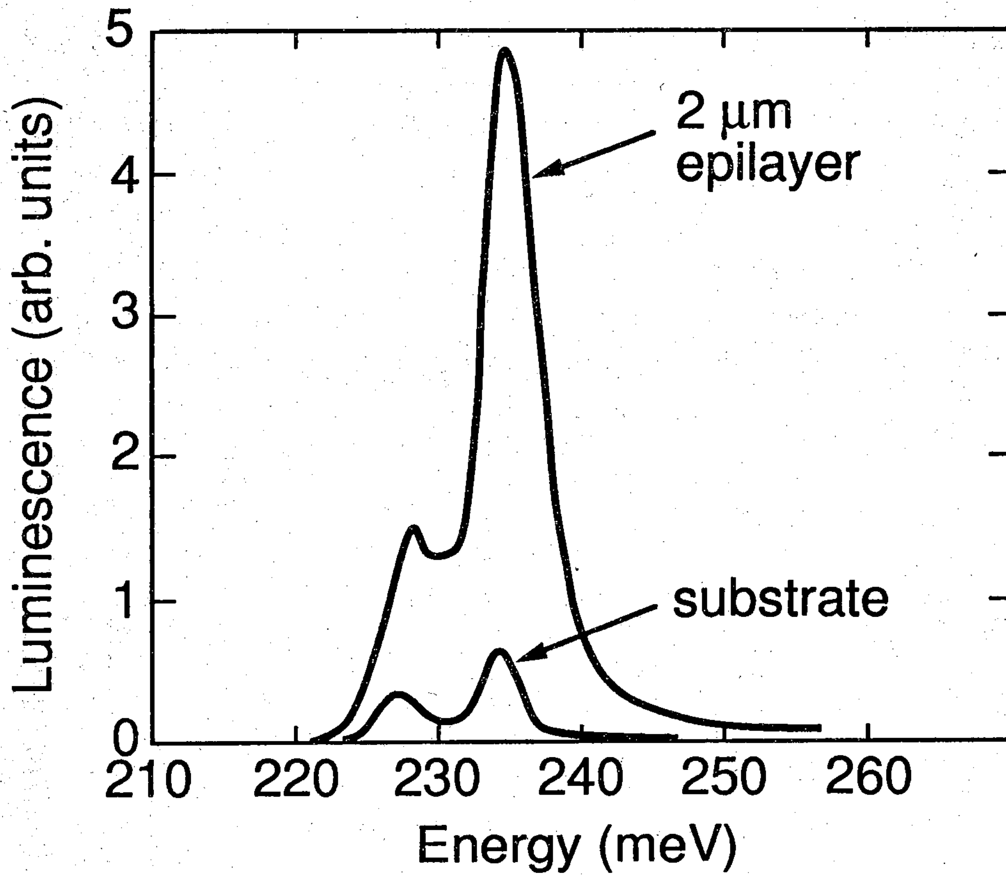

Figure 3.6 Photoluminescence spectra of a 2μm (100) InSb epilayer and InSb substrate.

momentarily interrupting impingement of the InSb and indium sources. The $(2\sqrt{2} \times 2\sqrt{2})45^\circ$ RHEED pattern was always seen to fade back to the diminished RHEED pattern after resuming the growth process. Diminished RHEED pattern intensity has been observed during the growth of a $2\mu m$ InSb layer demonstrating identical DCRC and TEM characteristics to that of an InSb substrate (as presented earlier). This suggests that, despite the non-optimal appearance of the RHEED pattern, the crystal formation process appears to be proceeding satisfactorily.

3.4 Conclusions

In conclusion, this section has presented details of the growth and characterization of InSb homoepilayers. The investigation of these layers for structural and optical properties has indicated two main points. First, InSb layers grown on InSb substrates have demonstrated excellent structural quality as judged by DCRC and TEM techniques. The use of these layers as a base for epitaxy of CdTe layers, therefore, appears promising. Second, the peak radiative intensity of epitaxial layers has been shown to exceed that of the bulk suggesting an enhanced quantum efficiency for the grown InSb layers. The use of this InSb material in CdTe/InSb/CdTe heterostructures would also seem to hold promise for the emission of radiation. Further, several criteria have been established for the evaluation of CdTe/InSb heterostructures in comparing the quality of heteroepitaxial InSb layers to the homoepitaxial variety.

CHAPTER 4
DUAL CHAMBER HETEROEPITAXY of (100) InSb - CdTe

With the successful growth of homoepitaxial InSb layers on InSb substrates (as described in chapter 3), the use of these layers for the growth of epitaxial CdTe is promising. As part of an effort to explore the growth of multilayer CdTe/InSb heterostructures, single CdTe films have been grown on InSb homoepilayers for independent study. Following completion of these studies, the growth of CdTe/InSb double heterostructures was undertaken. For growth of double heterostructures, as for the growth of single CdTe epilayers on InSb epilayers, separated MBE chambers have been utilized to grow InSb and CdTe layers. An ultrahigh vacuum (10^{-10} Torr) transfer module was utilized for the transfer of the sample block between growth chambers. TEM, DCRC, PL, and Raman scattering techniques have been utilized for analysis of heterostructures.

4.1 (100) CdTe / InSb Single Heterostructures

4.1.1 Transferral of InSb Epilayers

After the growth of InSb epilayers on InSb substrates, the sample temperature was reduced from the growth temperature of 300 °C to 250 °C and the sample was transferred from the InSb chamber to the CdTe growth chamber. The sample transferral process, involving the movement of the sample block from the InSb chamber through an ultrahigh vacuum transfer tube and into the CdTe growth chamber, was accomplished within several minutes. During the transfer, the sample was not heated. Upon arrival in the CdTe chamber, the InSb epilayers were heated to 200 °C with the surface of the sample facing away from the closed CdTe source oven. After stabilizing the sample temperature at 200 °C, the samples were brought into the growth

position and observed by RHEED. For InSb layers exhibiting intense RHEED patterns in the InSb chamber prior to transferral, RHEED patterns for transferred layers were often seen to exhibit a $(2\sqrt{2} \times 2\sqrt{2})45^\circ$ reconstructed InSb surface. Other films were seen to exhibit only integral order (bulk) RHEED streaks. (InSb layers were not passivated with a protective material for transferral.) Final calibration of substrate temperature was achieved, for some films, by measuring the InSb film surface temperature in the CdTe chamber with an infrared pyrometer [35]. In these cases, calibration of the pyrometer was achieved by measuring the InSb film surface temperature in the InSb chamber immediately after growth of the layer.

4.1.2 Growth of CdTe/InSb

Growth of the CdTe layers was accomplished by means of a single CdTe source oven containing polycrystalline CdTe. The early stages of epitaxy were seen to occur by the conversion of the InSb RHEED pattern to a CdTe pattern exhibiting (2x1) tellurium-stabilized reconstruction [39]. After several minutes of growth at 200 °C, the substrate temperature was raised from 200 °C to 240 °C by 1 °C per minute. (This procedure is similar to a procedure used by Williams et al. [8] where CdTe films were nucleated on InSb at 200 °C and raised to higher temperatures for growth). Growth at 240 °C was usually characterized by retention of the (2x1) reconstructed CdTe surface by RHEED observation. Figure 4.1 shows typical CdTe RHEED patterns observed during the growth of a CdTe heteroepilayer. The CdTe source oven used for these film growths was a standard PBN crucible with a thin PBN cap covering the CdTe source charge. Flux from the CdTe oven was evolved through a 1/8 inch hole in the center of the PBN cap. A temperature of 670 °C was typically used for the CdTe source oven, during growth, to produce a growth rate of 1 Å/sec.

4.1.3 Structural Analysis

Examination of CdTe/InSb heteroepitaxial structures has been performed by TEM and DCRC techniques. Cross-sectional TEM samples have been prepared by argon ion thinning in a similar manner to that described in

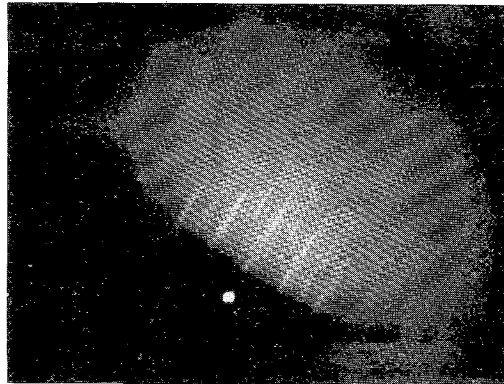

(a)

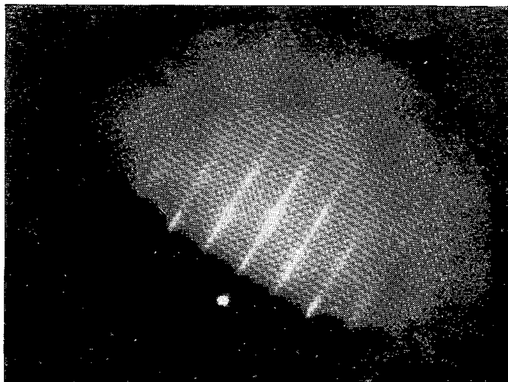

(b)

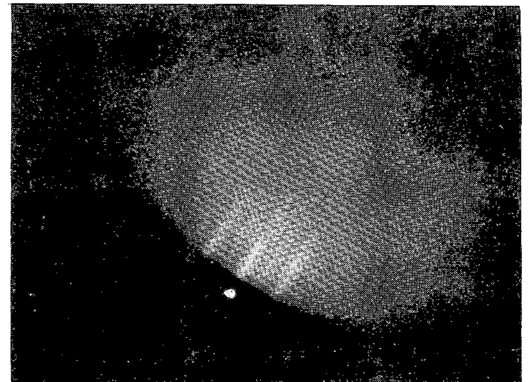

(c)

Figure 4.1 RHEED patterns for the growth of (100) CdTe on a (100) InSb epitaxial layer: (a) InSb epilayer [$\bar{1}10$] after transfer to the CdTe chamber, and CdTe layer during growth (t = 35 min) in the (b) [$\bar{1}10$] and (c) [110] directions.

chapter 3. The tendency for InSb to be sputtered at a faster rate than CdTe has lead to a great deal of difficulty in preparation of these TEM samples. Iodine thinning has been utilized by other workers [40] in the final milling step and has tended to reduce the formation of defects caused by the thinning process. Subsequently, iodine thinning has been utilized in the final milling step on a number of heterostructural samples and improvements in the quality of TEM samples have been achieved. A 200 kV high resolution electron micrograph HREM image of a CdTe/InSb heterointerface is shown for the [100] direction in Figure 4.2. The [100] projection allows for observation of chemical dissimilarities between the InSb and CdTe layers unlike the [110] projection. In the HREM image shown here, the (220) fringes from InSb and CdTe layers differ greatly, thereby revealing the interface [11]. For further insight into the structural quality of CdTe epilayers, DCRC scans have been performed. Diffraction peaks from the CdTe epilayer were found to have FWHM values of 40 arc seconds as shown in Figure 4.3.

4.1.4 Optical Analysis

4.1.4.1 Photoluminescence

To investigate the optical properties of CdTe epilayers, photoluminescence measurements have been performed. Excitation from an argon laser at 5145Å was focussed to a 500μm spot on CdTe films which were mounted in a liquid helium cryostat. A 0.75 m SPEX monochromator was utilized to collect the luminescence spectra and channel it to a cooled (-20 °C) GaAs photomultiplier tube. The 8K photoluminescence from a 1.3μm thick CdTe epilayer, grown at 240 °C, is shown in Figure 4.4. Under 230 mW/cm^2 excitation, Figure 4.4a shows competition between near band-edge features and impurity-band features for the recombination of electron hole pairs. Excitation under a more modest power of 1.68 W/cm^2 is shown in Figure 4.4b, while a magnification of the near band-edge region is shown in Figure 4.5.

For the near band-edge spectrum, the (n=1) free exciton transition, at 1.596 eV, appears to dominate the luminescence spectrum [5,28,41]. We also observe a weak feature at 1.6034eV which appears to be the (n=2) second

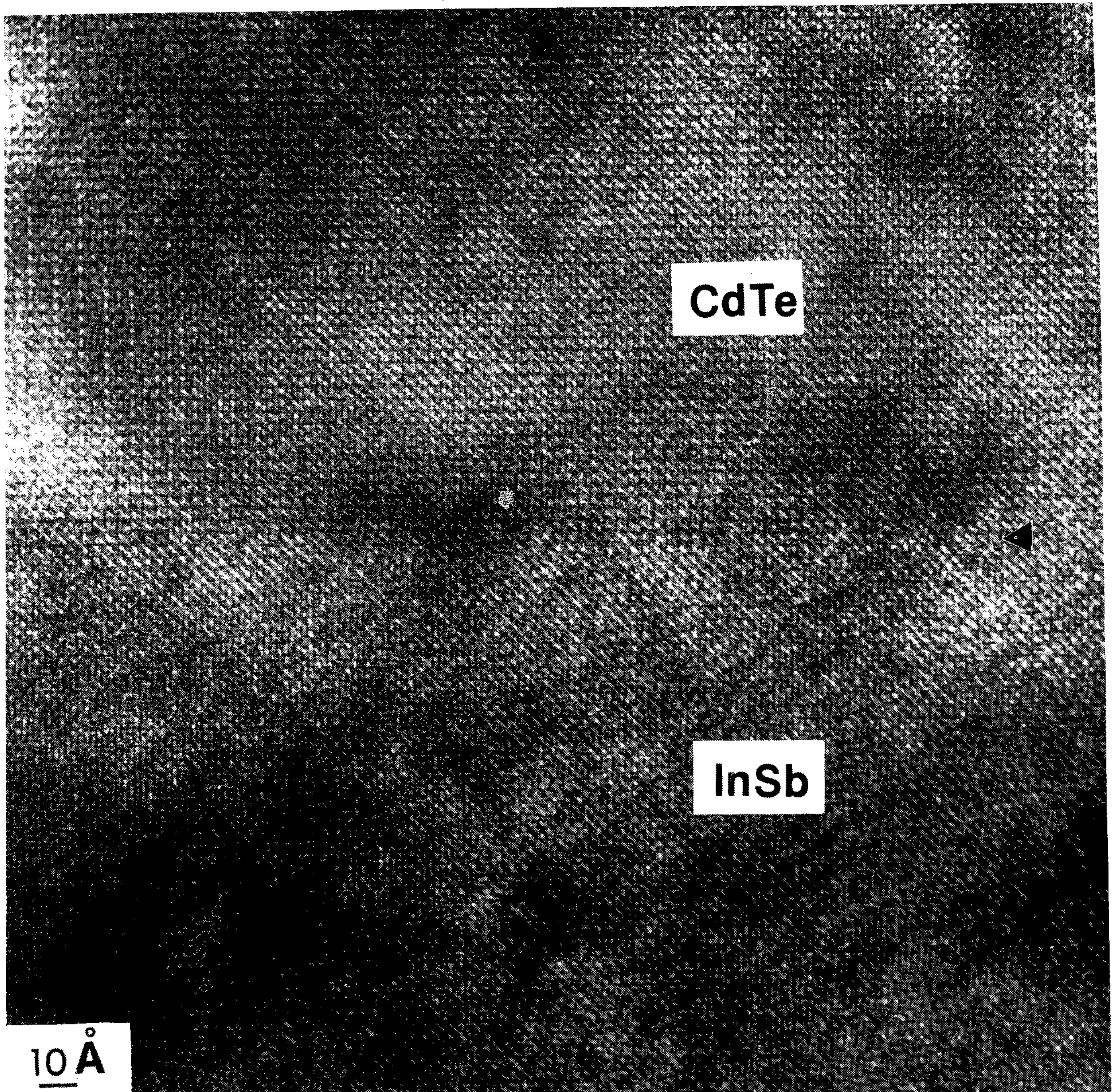

Figure 4.2 Cross-sectional TEM (200 kV) high resolution electron micrograph of a CdTe/InSb epilayer interface in the [100] projection.

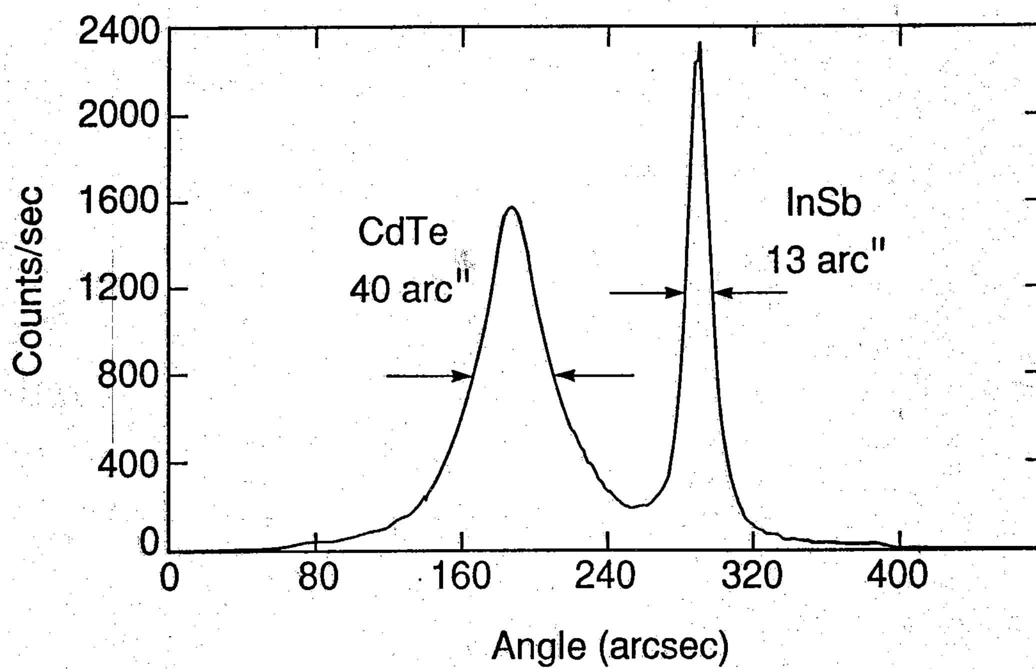

Figure 4.3 (004) X-ray DCRC trace of a 1.3μm CdTe layer on a 0.5μm InSb homoepitaxial layer.

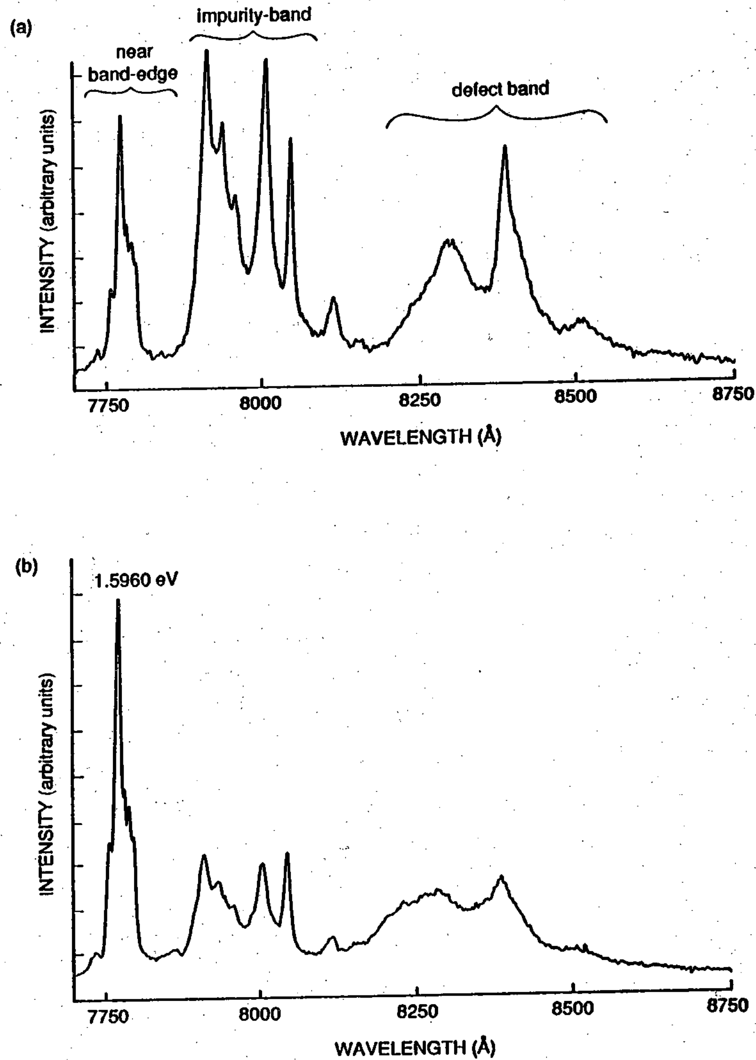

Figure 4.4 Low temperature (8 K) photoluminescence of a 1.3μm CdTe epilayer grown on an InSb epilayer. Excitation conditions are (a) power density = 1.68 W/cm^2 and (b) power density = 230 mW/cm^2. Dominant band-edge feature is free exciton (n=1) at 1.596 eV.

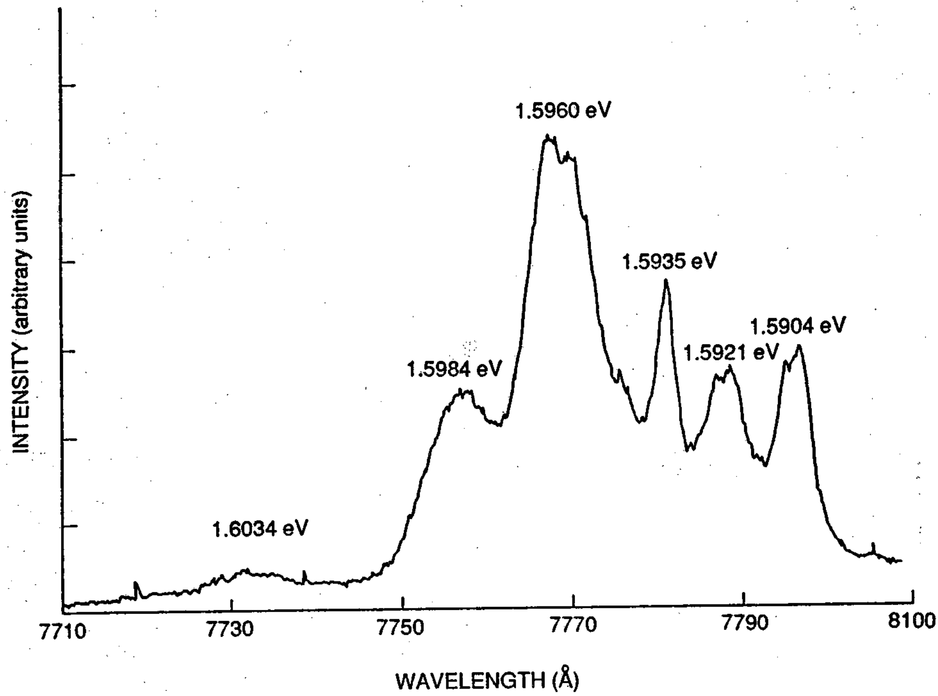

Figure 4.5 Low temperature (8 K) photoluminescence of a 1.3μm CdTe epilayer grown on an InSb epilayer (as shown in Figure 4.4). Near band-edge features at: 1.596 eV (n=1) free exciton, 1.5984 eV (polariton), 1.6034 eV (n=2) free exciton.

excited state of the free exciton, reported previously for (100) CdTe/InSb [5,41]. The peak at 1.5984 eV has also been reported for (100) CdTe/InSb and was previously assigned to the upper polariton branch of a free exciton [41]. Other features in the PL spectra have been tentatively identified as an acceptor bound exciton (A,X) at 1.5903 eV [41], and an ionized donor bound exciton (D^+,X) at 1.5921 eV [5]. The features 1.5935 eV is in the range (1.593eV) where neutral donor bound excitons have been reported for CdTe. Feng et al. [41] have recently reported that a feature at 1.5931eV, seen in (100) CdTe/InSb, is not due to a simple donor bound exciton but may be related to a donor-like defect in the film structure or an impurity-defect complex.

4.1.4.2 Modulated Reflectance

To give additional insight into the band-edge optical nature of CdTe epilayers, piezomodulated reflectance has been performed by Lee et al. [42]. Here, a lead-zirconate-titanate transducer driven by a sinusoidal electric field was used to excite the sample. A lock-in amplifier was used for detection of the reflectance signal through a Perkin Elmer (E-1) monochromator. The piezomodulated reflectance spectrum for a 1.3μm CdTe epilayer is shown in Figure 4.6. As in the photoluminescence measurements (Figure 4.5), a dominant free exciton feature is observed in the reflectance spectra along with other near band-edge features of lesser intensity. The upper branch polariton feature, seen at 1.5984 eV in the PL spectra is also identified in the modulated reflectance spectra at 1.5983 eV. As observed by Lee et al. [42], the polariton feature has also been observed in the spectra of very high purity CdTe bulk material [43] and has been identified as an indication of high structural quality.

4.2 (100) CdTe / InSb Double Heterostructures

Following the successful growth of single CdTe epilayers on InSb homoepilayers, double InSb/CdTe heterostructures were grown. The growth of double heterostructures was achieved by extending the substrate transferral process, used for the growth of single heterostructures, to the addition of an

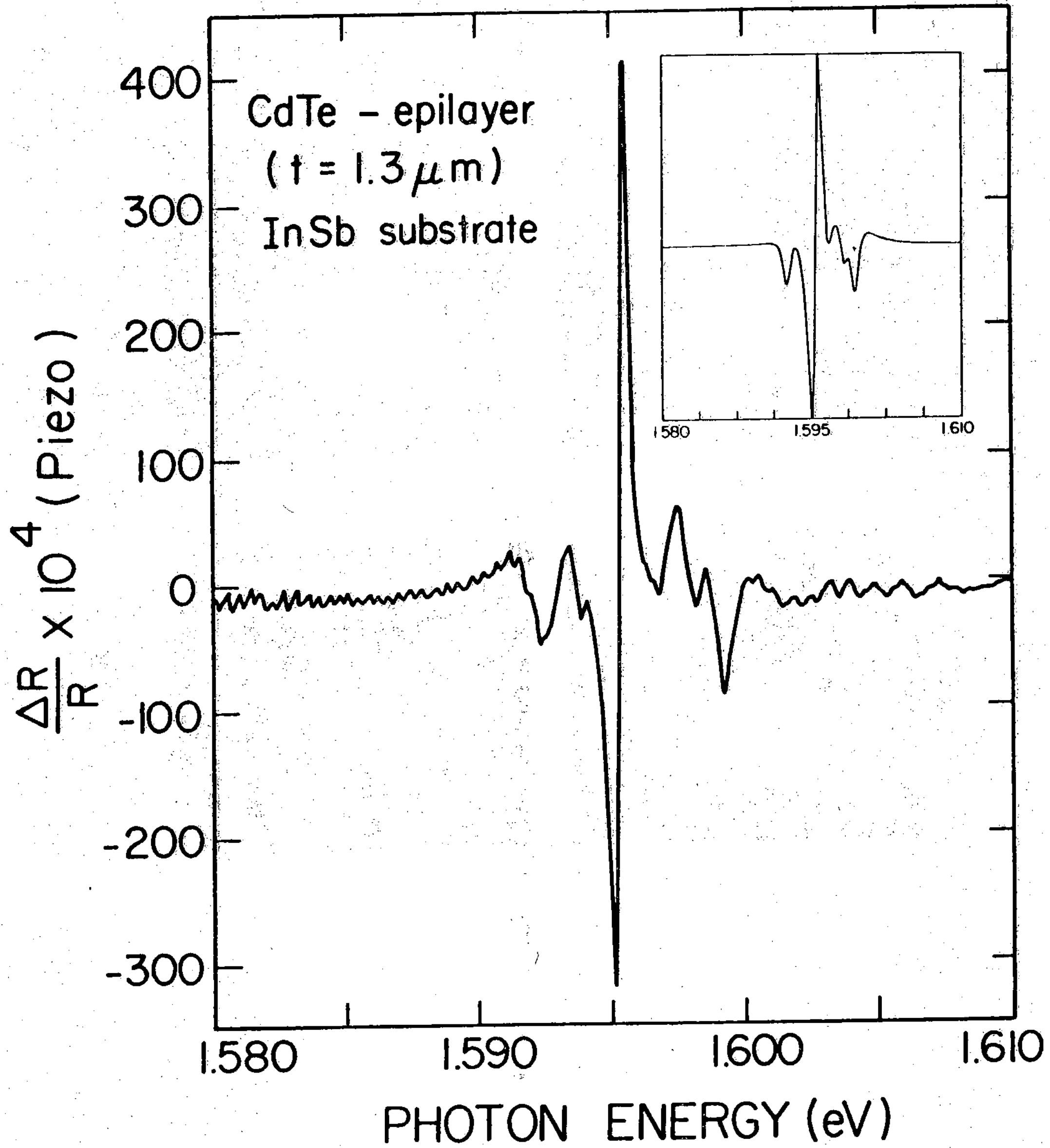

Figure 4.6 Piezomodulated reflectivity spectrum of a 1.3μm CdTe epilayer grown on an InSb epilayer. Inset: Theoretical fitting to the first derivative of a Lorentzian function. Reprinted from Lee et al. [42].

InSb active layer and CdTe capping layer. After growth of the InSb and CdTe "buffer" layers, the sample would be transferred through ultra-high vacuum from the CdTe growth chamber to the InSb growth chamber. Upon arrival at the InSb chamber, the sample would be heated to the growth temperature (300 - 330 ° C) and allowed to stabilize. At this point, the sample would be brought into the growth position and observed by RHEED. A comparison of RHEED patterns for the CdTe layer before and after transferral indicates that the surface reconstruction features have not significantly changed as a result of the transfer process.

4.2.1 Growth of InSb and CdTe layers

Nucleation of heteroepitaxial InSb films was achieved, as for the homoepilayers, by opening the InSb and indium source shutters. A very dramatic change was instantly observed in the RHEED pattern with the formation of spots throughout the entire RHEED screen. The spotty RHEED pattern, which indicates a three-dimensional nucleation mechanism, was seen to evolve into a streaked pattern within approximately 75 seconds (growth rate = 1Å/sec). RHEED photos for the nucleation and growth of a 160Å InSb layer on a transferred CdTe "buffer" layer are shown in Figure 4.7. For the growth of the InSb active layers, the expected $(2\sqrt{2} \times 2\sqrt{2})45^\circ$ RHEED pattern was observed shortly after nucleation of InSb on CdTe and was seen to persist throughout the growth of InSb layers (at least up to a thickness of 5600Å/sec). The intensity of the RHEED images was typically lower for the growth of heteroepitaxial InSb layers than for the growth of homoepitaxial InSb layers. As was observed for InSb homoepilayers, the intensity of the RHEED patterns for heteroepilayers was seen to increase after the termination of growth.

Following the completion of InSb layer growth, the InSb substrate temperature was immediately reduced, and upon reaching 250 ° C, the sample was transferred, in vacuum, to the CdTe chamber. In the CdTe chamber, the InSb film would be heated to 240 ° C for the growth of a CdTe capping layer. The sample temperature was set to 240 ° C (and not 200 ° C) for nucleation of the CdTe layer as the growth period for the layer was short ($\simeq$ 34 minutes).

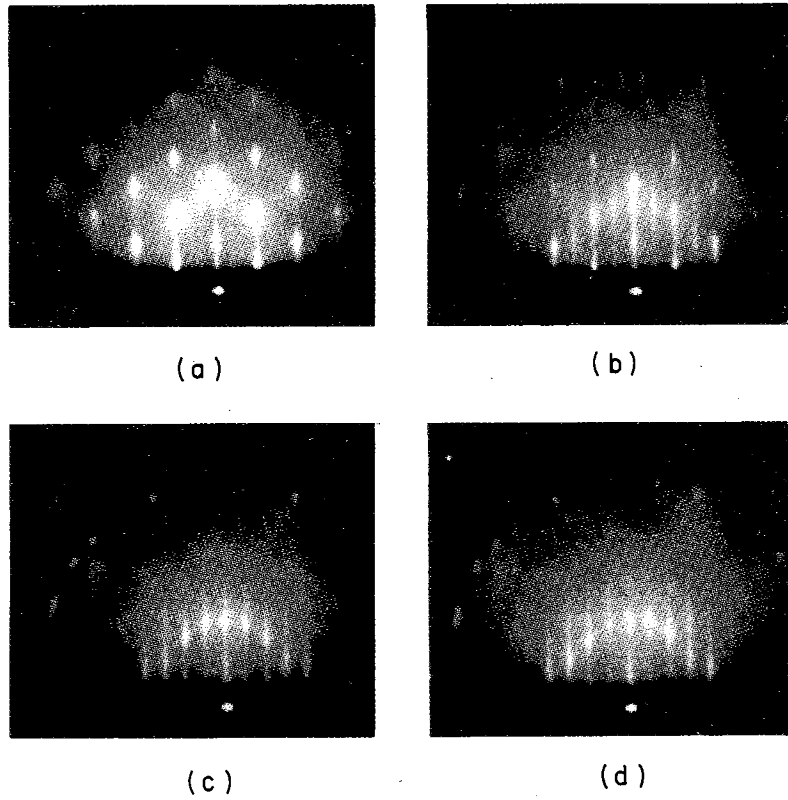

Figure 4.7 RHEED patterns observed during the growth of an InSb (160Å) quantum well structure: (a) t = 5 sec, (b) t = 75 sec, (c) t = 115 sec, and (d) after film growth (t = 152 sec).

Growth of the CdTe film was again performed by means of a single CdTe effusion source at a rate of 1 Å/sec. Upon nucleation, the RHEED pattern was seen to remain streaked, but was seen to evolve into the CdTe RHEED pattern. CdTe capping layers were typically 2000 - 2200Å in thickness. CdTe layer growth was ended by closing the CdTe source oven shutter, and reducing the sample temperature.

4.2.2 Structural Analysis

Structural analysis for CdTe/InSb heterostructures has been performed by TEM. A dark field TEM micrograph for an InSb (160Å) quantum well structure is shown in Figure 4.8. The structure consists of a 0.5μm InSb epilayer on InSb substrate, a 1.53μm CdTe buffer layer, the InSb active layer, and a 0.21μm CdTe capping layer [15]. The InSb layer is shown as dark contrast with the CdTe layer showing up as a light contrast in the micrograph. Closer examination of double heterostructures by TEM cross sectional micrographs has indicated that the CdTe-InSb heterointerfaces are planar (flat) across the layer. The presence of interfacial mixing layers, such as In_2Te_3, reported to be of tens of angstroms in thickness [19], and segregated antimony are expected to be visible by TEM analysis. As yet, the existence of a mixed interface has not been confirmed in the TEM samples examined here. Further study into the existence of these layers through TEM analysis will be pursued.

4.2.3 Optical Analysis

Infrared photoluminescence data has been taken at 10K with a YAG laser and cooled (77K) InSb infrared detector. The luminescence from a 5600Å InSb active layer, confined between CdTe layers, is plotted with the luminescence from an InSb substrate in Figure 4.9. In this case, the double heterostructure is based on an InSb substrate with a 0.42Å InSb epitaxial layer, a 1.63μm CdTe buffer layer, the InSb active layer, and a 0.22μm CdTe capping layer. Two peaks are seen in the luminescence spectra for the heterostructure, with the higher energy feature being attributed primarily to band-to-band recombination in the InSb layer [12,15,38]. Spectra for the

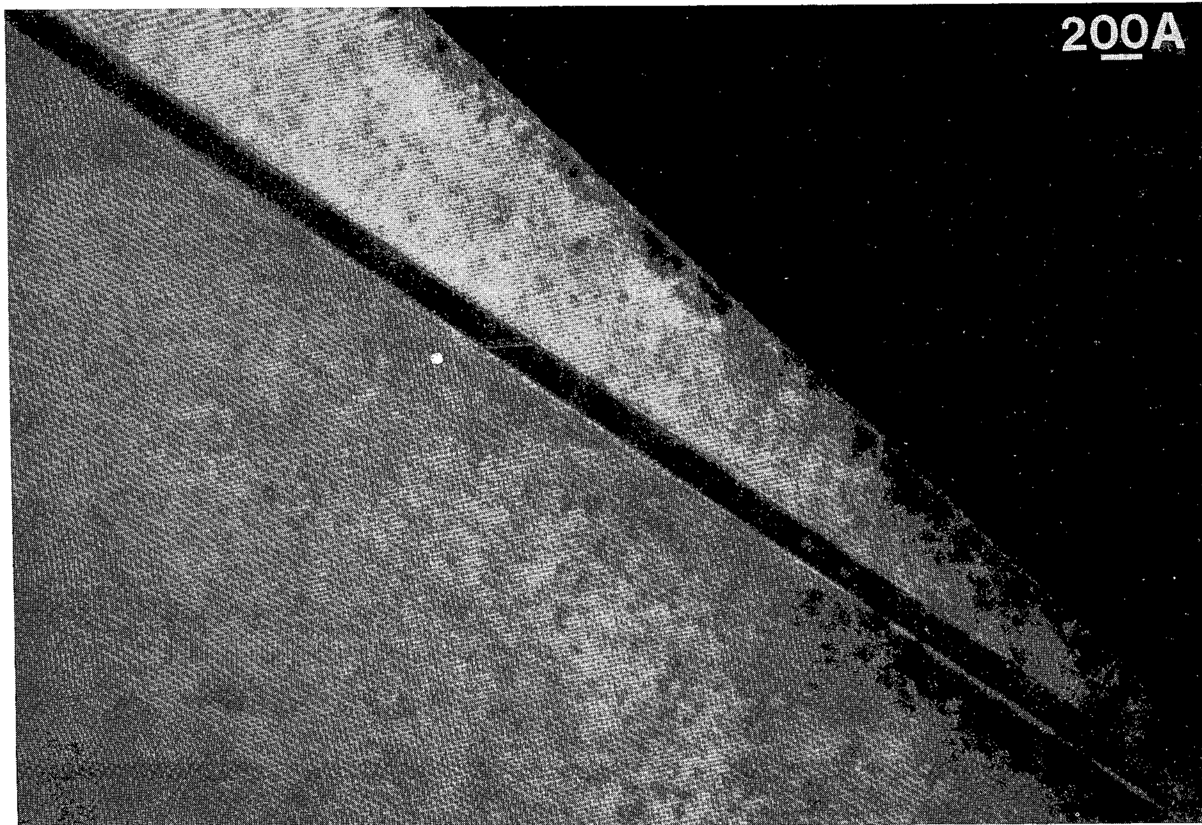

Figure 4.8 Cross-sectional dark field TEM micrograph of CdTe/InSb double heterostructure in the [110] projection. Dark stripe is the 160Å InSb single quantum well surrounded by CdTe (light contrast).

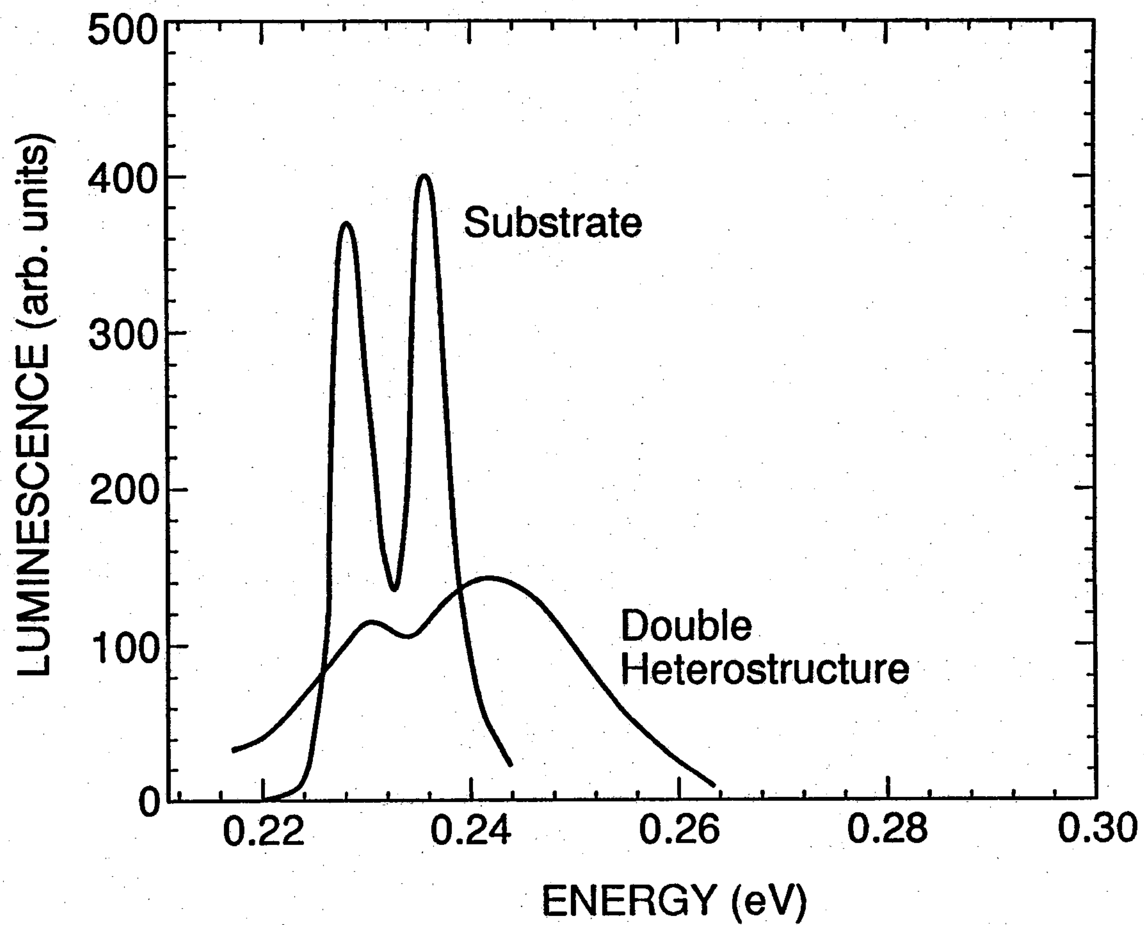

Figure 4.9 Low temperature (10K) infrared luminescence of an InSb active layer (5600Å), in double heterostructure configuration, compared to an InSb substrate.

double heterostructure is seen to be broader (to the high energy side) than that observed for the InSb substrate. It is difficult to attribute this high energy broadening to InSb or CdTe layers alone. At this time, the luminescence observed on the high energy side for this heterostructure has been attributed to recombination at interfacial regions. Further investigation of this phenomenon is being pursued by the use of Raman spectroscopy in addition to photoluminescence in an attempt to characterize the III-V/II-VI interfacial region.

4.3 Conclusions

For the fabrication of single and double InSb/CdTe heterostructures separate III-V and II-VI chambers have been utilized for the growth of InSb and CdTe layers. Material properties have been examined to determine the quality of structures grown by interrupted molecular beam epitaxy. TEM and RHEED have provided information which suggests that the growth of CdTe/InSb and InSb/CdTe could be accomplished, despite the transfer of samples between growth chambers. Photoluminescence from a double heterostructure has been shown to resemble that of an InSb substrate while being broader to the high energy side of the spectrum. The influence of possible interfacial layers on the properties observed is currently being explored.

CHAPTER 5
SINGLE CHAMBER HETEROEPITAXY of (100) InSb - CdTe

5.1 Overview

The growth of CdTe/InSb heterostructures in a single MBE growth chamber is described. In the previous chapter, a multichamber growth process was employed for the fabrication of CdTe/InSb heterostructures, whereby InSb and CdTe layers were grown in separate chambers. For the creation of multiple quantum well heterostructures, the process of transferring a sample block between III-V and II-VI growth chambers was deemed impractical. A single, CdTe-InSb, growth chamber was thus established by adding an antimony cracking furnace and elemental indium source to the chamber previously designated for the growth of CdTe layers. The antimony cracker was employed to explore the low temperature growth of InSb using Sb_2. Structures, grown with the use of the cracker, have been analyzed by TEM and DCRC measurements to determine their structural properties. Multilayer heterostructures have been grown which exhibit superlattice diffraction features when examined by DCRC techniques. New developments which have been made in the continuous heteroepitaxy of CdTe/InSb structures will be discussed in the ongoing efforts to produce multilayer quantum well structures.

Recently, there have been several reports concerning the growth and characterization of CdTe/InSb multilayer heterostructures [12-17]. In the work reported by Golding et al. [13], multilayer heterostructures were grown at 300 °C on InSb substrates. To address the problem of intermixing between CdTe and InSb layers, Golding et al. have employed the growth of CdTe layers in the presence of a cadmium overpressure ($J_{Cd}/J_{Te} = 3$). In the work presented here, the growth of CdTe/InSb heterostructures has been explored at substrate temperatures between 280 and 310 °C on both InSb and CdTe

substrates [12,14-16]. In light of previous reports citing several problems with the growth of InSb with substrate temperatures at or below 300 °C, the low temperature growth of InSb has been approached by utilizing very low growth rates ($<$ 0.4Å/sec) and Sb_2 from a cracking furnace. The cracker was chosen over the standard PBN effusion crucible for two main reasons. First, it was deemed necessary to experiment with the use of antimony dimer species to investigate its potential for growth of InSb films at low temperatures. The use of Sb_2 was motivated by experiments performed on the GaAs material system where it was reported [32,33] that the density of deep level electronic traps, in films grown at low temperatures, could be reduced by utilizing very low growth rates and As_2 rather than As_4. Second, it has been speculated that the migration of tellurium species into a cracking furnace would be a less likely than the migration of tellurium into a standard crucible. To further limit the migration of Te into the cracker, the cracking zone has been continuously maintained at elevated temperatures ($\geq$ 600 °C) and the LN_2 cryogenic shrouds have been kept at a temperature of 77K.

5.2 Setup

5.2.1 Use of Antimony Cracking Furnace

The antimony cracking furnace used in our work is diagramed in Figure 5.1. The unit is composed of a 120cc tantalum bulk evaporator and 0.5 inch diameter cracking tube. To remove residual contamination, the bulk evaporator (empty) was outgassed to 860 °C for 6 hours while the cracking zone was outgassed at 1380 °C for 1.5 hours then reduced to 1000 °C for 4.5 hours. Source material, consisting of 6N5 purity antimony, was then loaded into the cracker and the charge was outgassed at 600 °C for 4 hours. Concerns about a possible reaction between the tantalum bulk evaporator and the antimony source charge prevented us from raising the source temperature to the melting point of antimony (631 °C) [24]. To prepare an indium source, a 60cc oven and PBN crucible were outgassed at 1200 °C (empty), loaded with 6N pure indium, and outgassed at 820 °C for 4 hours.

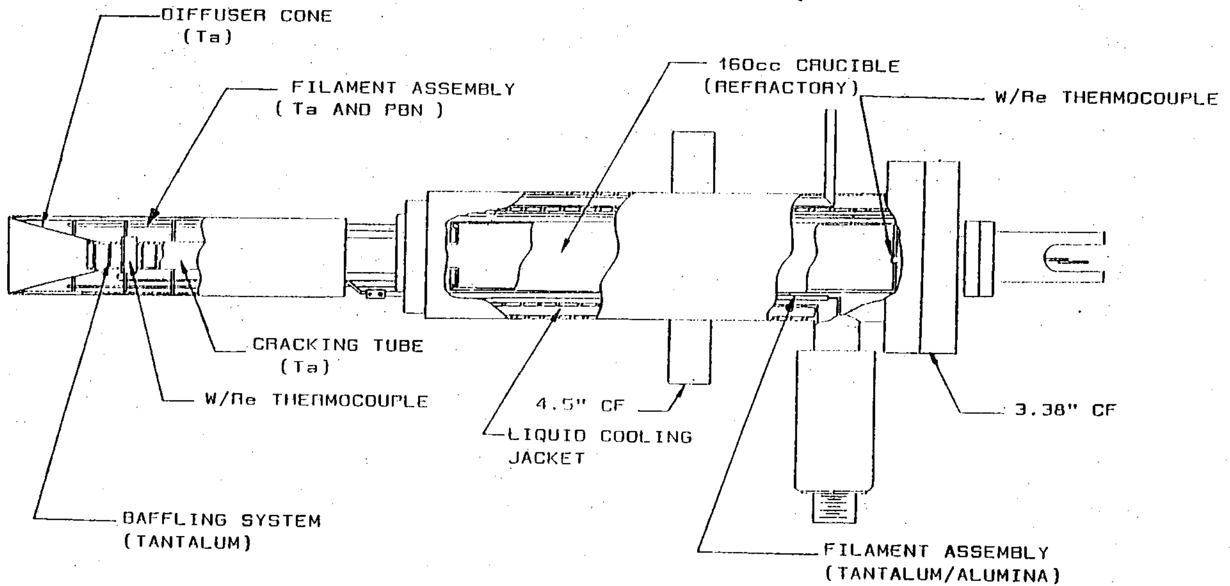

Figure 5.1. Schematic diagram of the antimony cracking furnace, supplied by EPI Systems. The cracker was used for growth of InSb in the dual III-V/II-VI growth chamber.

5.2.2 Substrate Preparation

For the growth of CdTe/InSb heterostructures in the single growth chamber, both InSb and CdTe substrates were utilized. InSb sample preparation has been described in chapter 3. CdTe substrates, purchased from Galtech Semiconductors, were examined for structural quality by performing multiple DCRC scans over the surface of each substrate. For the substrates examined, diffraction peaks were typically 20 - 30 arc seconds in width (FWHM). After DCRC analysis, the substrates were degreased in two cycles of boiling TCA and ultrasonically agitated in acetone and methanol. After drying in N_2 gas, the substrates were etched in 1% Br:MeOH for 60 seconds. Etching was halted by flushing the etchant with methanol for several minutes. Substrates were then dried with N_2 gas and mounted, with gallium, onto Mo sample holders [14,15]. For the purpose of calibrating the block temperature, a bead of indium (melting point at 156 $^\circ$C) was mounted beside each substrate. Sample holders were then placed in the sample introduction chamber and heated to 200 $^\circ$C for one hour to drive off water vapor.

5.3 Continuous Growth of InSb - CdTe Multilayers

5.3.1 Growth Process

The growth of homoepitaxial InSb buffer layers was accomplished using a nearly identical procedure as that described in chapter 3. After calibration of the block temperature using a Au:Ge eutectic, oxide desorption was accomplished by raising the InSb substrate temperature while observing RHEED patterns from the InSb substrate. When the oxide layer was beginning to desorb, a flux of antimony, in this case from the cracker, was initiated. As for homoepilayers grown in the InSb machine, complete oxide desorption was signaled by a significant reduction in the background scattering observed on the RHEED screen and an intensifying of the InSb RHEED pattern. Once the oxide was believed to be removed, the substrate temperature was reduced, and the antimony flux discontinued. Nucleation of the InSb layer was achieved by opening the antimony cracker and indium oven shutters simultaneously at a substrate thermocouple reading 25 $^\circ$C above the desired growth temperature. For growth of InSb epilayers, a substrate

temperature of 330 °C was used along with a flux ratio (J_{Sb}/J_{In}) of approximately unity. An antimony-stabilized ($2\sqrt{2}$ x $2\sqrt{2}$)45° RHEED pattern was typically observed during film growth.

Prior to completion of the InSb buffer layer, the substrate temperature was reduced from 330 °C to 300 °C. Upon reaching 300 °C, the InSb film growth was terminated and the substrate temperature reduced to 200 °C for the nucleation of a CdTe buffer layer. After the nucleation of CdTe at 200 °C, the substrate temperature was raised by 1 °C/min to a growth temperature of 240 °C [14,15]. CdTe substrates were prepared for epitaxy by *in-situ* heating to between 325 and 370 °C, followed by immediately reducing the substrate temperature to 200 °C. At 200 °C, CdTe buffer layers were nucleated and the substrate temperature stepped up by 1 °C/min to a growth temperature of 240 °C. During growth of CdTe layers on InSb epilayers or CdTe substrates, a (2 x 1) reconstruction pattern, characteristic of a Te-stabilized surface [39], was typically observed by RHEED [15].

Before the end of CdTe buffer layer growth ($\simeq$ 1μm), on either substrate type, the substrate temperature was raised from 240 °C to 280 °C at a rate of 2 °C/min. After a short stabilization period, growth of InSb/CdTe multilayer structures was commenced without interruption of epitaxy, by closing the CdTe shutter and opening the antimony cracker and indium source shutters. In every case, InSb layers were seen to nucleate in a three-dimensional fashion on CdTe, as suggested by the observation of a spotty RHEED pattern. In contrast, growth of CdTe layers on InSb was seen to occur by the formation of streaks in the [100] and [$1\bar{1}0$] RHEED patterns which persisted throughout growth. Following the completion of multilayer growth, a 500Å CdTe capping layer was typically grown to protect the structure.

5.3.2 Structural Analysis

Several multiple quantum well structures have been grown with antimony cracking zone temperatures of 850 °C and 1040 °C, under otherwise similar growth conditions. DCRC measurements for a multiple quantum well structure, grown with the lower antimony cracking zone temperature, show FWHM values of 32 arc seconds for the supporting CdTe buffer layer. Despite

having a high quality buffer layer, TEM micrographs have indicated that these structures exhibit a high density of dislocations which appear to form in the InSb multilayers. Figure 5.2 shows a bright field TEM micrograph of a multilayer structure grown with a cracking zone temperature of 850 ° C. By comparison, structures grown under the same conditions with the exception of a higher antimony cracking zone temperature, have shown a ten-fold decrease in the density of these dislocations. Figure 5.3 shows a dark field TEM micrograph of a multiple quantum well structure consisting of 167Å CdTe and 163Å InSb layers. The structure was grown with an antimony cracking zone temperature of 1040 ° C. Since the multiple quantum well structures were grown at 280 ° C, the reduction in dislocation density is speculated to be due to a reduction in the formation of antimony precipitates at these low growth temperatures. The exact correlation between the occurrence of defects in grown InSb layers and the temperature used to crack antimony is, however, uncertain.

5.3.3 Optical Analysis

Raman spectroscopy has been employed to explore the issue of a mixed interface by focusing on the optical phonon region of the spectrum. (Raman spectroscopy studies have been performed at Brown University by N. Pelekanos and T. Heyen under the direction of Dr. A. V. Nurmikko.) Typically, well resolved features resulting from bulk-like InSb LO phonons have been observed, even in the narrowest quantum well samples. Apart from these bulk-like LO-phonon features in the Raman spectra, occasional weak features have been observed (in certain isolated samples) which are apparently related to lattice vibrations reported [19] for chemically intermixed InSb/CdTe interfaces. For the majority of samples, such features, if present, are below our current level of detection. This issue is presently being brought under close scrutiny with respect to photoluminescence examinations, to explore any possible interrelationships.

Figure 5.2. Cross sectional TEM micrograph in the [110] direction showing a CdTe/InSb multilayer structure. The structure was grown at 280 ° C with an antimony cracking temperature of 850 ° C.

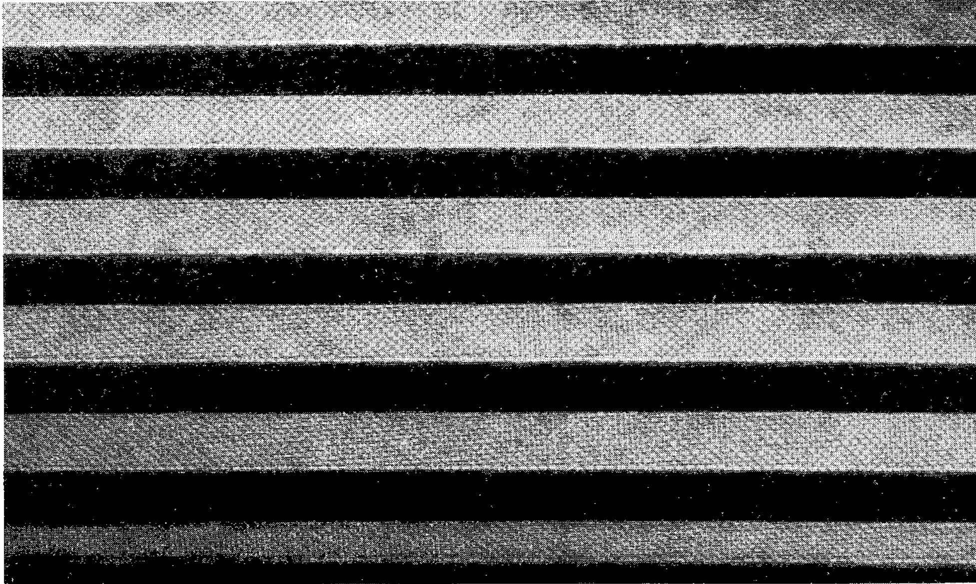

Figure 5.3. Cross sectional [110] TEM micrograph showing a CdTe/InSb multilayer structure grown with an antimony cracking temperature of 1040 ° C. Light contrast regions are the 167Å CdTe layers and dark contrast regions are the 163Å InSb layers..

5.4 Interrupted Growth of InSb - CdTe Multilayers

5.4.1 Growth Process

In a recent set of experiments, multilayer CdTe/InSb heterostructures have been grown at substrate temperatures in the range of 310 °C. To examine the material properties of CdTe grown at these temperatures, single InSb and CdTe epitaxial layers were grown at 310 °C and examined by x-ray rocking curve measurements. InSb layers of approximately 1μm in thickness have been examined by DCRC measurements and were found to resemble single InSb epilayers grown (without the cracker) in the isolated InSb chamber (chapter 3). Figure 5.4 shows an (004) x-ray DCRC diffraction pattern for a 1μm CdTe layer grown at 310 °C with a rate of 0.4Å/sec [15,16]. In this case, the x-ray diffractometer was equipped with a four-pass silicon monochromator instead of the conventional single-pass InSb monochromator. As can be seen, the CdTe layer has a FWHM value of 17 arc seconds while the supporting InSb epilayer/substrate crystal has a FWHM value of 12 arc seconds. Also shown in the figure, are an array of periodic, low intensity diffraction features, located between the InSb and CdTe diffraction peaks. These peaks have been attributed to the interference between x-ray waves reflected from the surface of the CdTe layer and from the CdTe/InSb heterointerface. The occurrence of these features has been interpreted as an indication of very high structural uniformity in the grown CdTe layer as well as an atomically flat CdTe/InSb interfacial region [44,45].

In addition to the multilyers grown at a substrate temperature of 280 °C, we have grown CdTe/InSb multilayer structures at 310 °C [16]. InSb substrates were used as a base for these structures upon which InSb and CdTe buffer layers were grown. Following the completion of CdTe buffer layer growth, the multilayer sequence was commenced. As for growth of the buffer layers, the InSb and CdTe multilayers were grown at a substrate temperature of 310 °C using an antimony cracking temperature of 1040 °C. For these films, the InSb and CdTe layers were grown at less than 0.4 Å/second. To allow for a partial relaxation of each InSb or CdTe layer surface, growth interruption periods of 12 seconds, for InSb, and 6 seconds, for CdTe, were used [16].

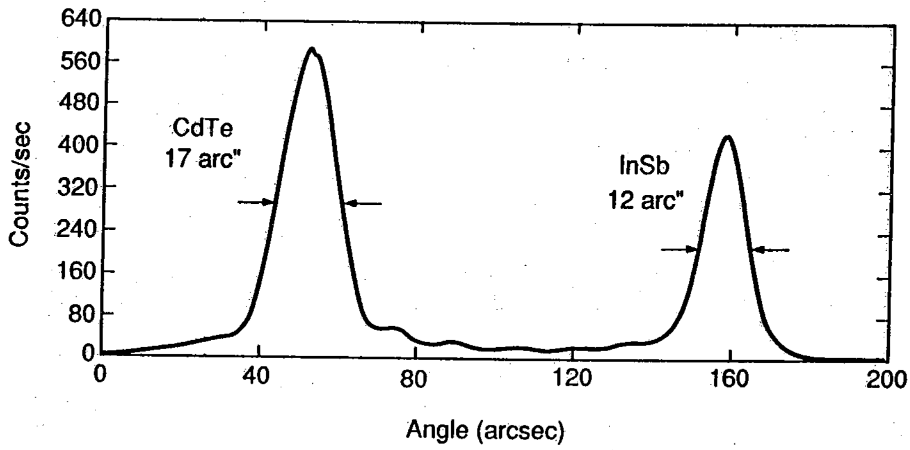

Figure 5.4. X-ray DCRC scan (004) of a 1μm CdTe epilayer grown on an InSb epilayer at 310°C. Scan was taken using a four-pass Si monochromator.

5.4.2 Structural Analysis

Figure 5.5 shows the DCRC scan for a 15 period multilayer structure grown at 310 °C [16]. Due to its high intensity and angular narrowness (11 arc seconds), the feature labeled "InSb" has been attributed to diffraction from the InSb substrate and buffer layer. Accordingly, the feature labeled "0", with a FWHM value of 22 arc seconds, has been attributed to the zero-order reflection from the CdTe-InSb multilayer [16]. A periodic array of satellite peaks, with a spacing of approximately 208 arc seconds, can be identified (±1, ±2) in symmetric angular arrangement about the feature labeled "0". The spacing of these satellite features corresponds to an average CdTe-InSb superlattice period of approximately 870Å. Analysis by TEM micrographs has indicated that the structure has an average superlattice period of 883 ±10Å.

Despite these results, there appears to be a discrepancy in the positioning of the features labeled "InSb" and "0" for the x-ray diffraction pattern shown in Figure 5.5 [16]. Since the growth-directed (a_z) plane spacing for the InSb substrate/buffer crystal should be smaller than the average lattice plane spacing associated with the periodic structure, the feature labeled "InSb" should appear at a higher Bragg angle than the feature labeled "0". Preliminary calculations [45], involving the minimization of strain energy in the multilayer region, have been used to account for the observed diffraction features when several monolayers of zincblende In_2Te_3 were assumed to be present in each CdTe/InSb multilayer period. In this model, it has been assumed that the In_2Te_3 layers could be incorporated at one or both of the heterointerfaces in some regular fashion. For the calculation, a value of 6.14Å has been assumed for the unstrained In_2Te_3 lattice parameter [46]. Elastic constant for these layers have been taken to be an average of the elastic constants for CdTe and InSb. A closer examination of the interfacial regions in these samples is in progress using high resolution (HREM) imaging in an attempt to isolate any such interfacial compounds.

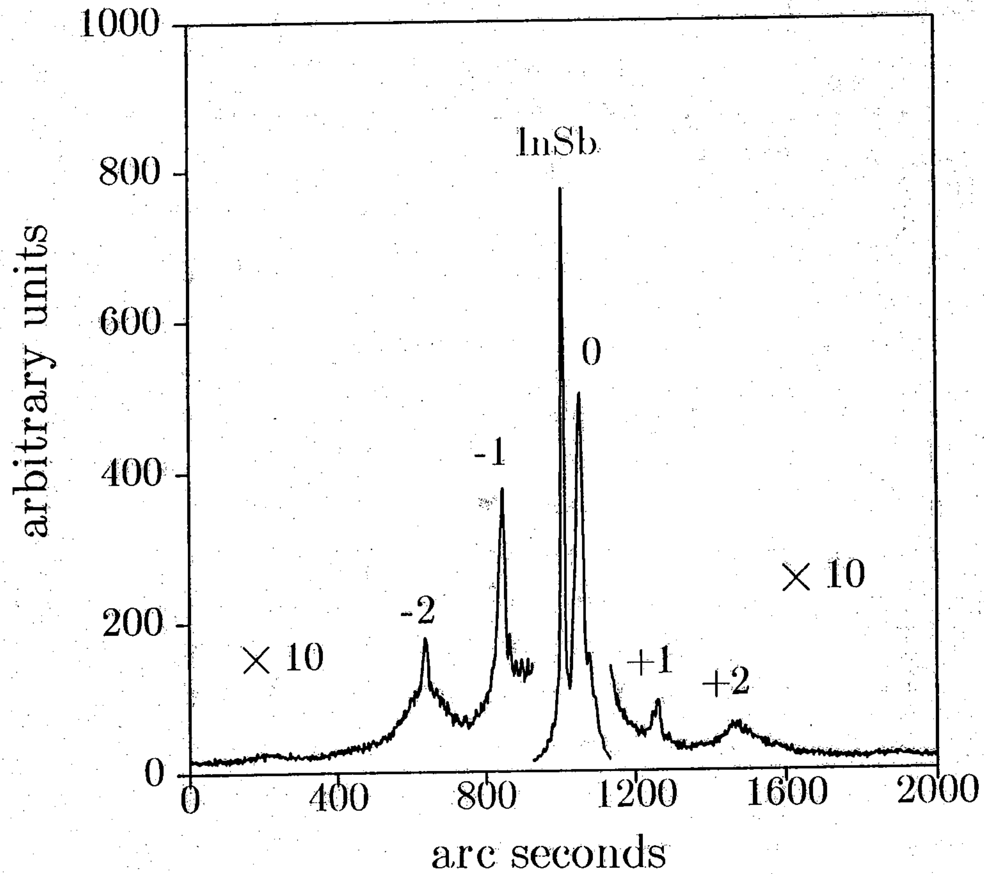

Figure 5.5. X-ray DCRC scan (004) of a 15 period CdTe/InSb multilayer heterostructure grown at a substrate temperature of 310 °C. Feature "InSb" is attributed to the InSb substrate, feature "0" is attributed to the primary diffraction from the multilayer region and features "±1" and "±2" are attributed to diffraction satellites from feature "0".

5.5 Conclusions

In conclusion, the growth and characterization of InSb/CdTe multilayer heterostructures has been described. For the work presented here, the InSb and CdTe layers were grown in a single MBE chamber with the antimony (for InSb layer growth) being supplied by a cracking furnace. Examination of heterostructures using TEM, DCRC and Raman spectroscopy has been described. TEM analysis has indicated that the formation of dislocations in InSb layers grown at a substrate temperature of 280 °C may have a dependence on the antimony cracking zone temperature used. Analysis of single InSb and CdTe epitaxial layers has indicated that high structural quality, indicated by narrow and symmetric DCRC diffraction peaks, may be achieved for layers grown at temperatures near 300 °C. Examination of multilayer heterostructures by the DCRC technique has also indicated the existence of satellite fringes which appear to originate from a periodic CdTe/InSb heterostructure.

CHAPTER 6
SUMMARY AND FUTURE RESEARCH

To summarize this report, InSb-CdTe single and multiple layered heterostructures have been successfully grown by molecular beam epitaxy. For the growth of these structures, two techniques have been employed. First, InSb and CdTe layers were grown in separate chambers to avoid the problem of cross-doping between III-V and II-VI material systems. InSb-CdTe double heterostructures were fabricated by transferring the sample block between III-V and II-VI chambers through an ultra-high vacuum transfer module. Alternatively, InSb and CdTe layers were grown in a single chamber, where an antimony cracker was utilized for the growth of InSb layers. With this procedure, multilayer heterostructures of up to 20 periods were grown.

Infrared photoluminescence and x-ray DCRC techniques have shown that the optical and structural properties of homoepitaxial InSb layers appear to be as good or better than that of InSb bulk material. Infrared photoluminescence of double heterostructures, grown using two chambers, has indicated that heteroepitaxial InSb layers can exhibit bulk-like band-to-band emission with some additional broadening to the high energy side. TEM and HREM micrographs indicate that double heterostructures may be grown which exhibit good structural quality despite the growth of III-V and II-VI layers in separate chambers.

With the need to grow multilayer heterostructures in a single MBE chamber, an antimony cracker was added to the II-VI growth chamber and used for the homo- and hetero-epitaxy of InSb. Multilayer heterostructures were grown using very low growth rates and substrate temperatures near 300 °C. These procedures were used in an attempt to (i) limit any possible interfacial mixing of the materials and (ii) grow the InSb and CdTe layers at a

mutually compatible substrate temperature. Examination of multilayer structures using TEM has indicated that the formation of defects in InSb films may be a function of the antimony cracking temperature used. Evidence for superlattice periodicity in multilayers grown with long period lengths has been indicated by multiple satellite peaks in x-ray DCRC measurements.

The ultimate goal of this project was to achieve quantum confinement in InSb/CdTe quantum well structures. Although falling short of this goal, the work presented here has made significant contributions to understanding the nature of CdTe/InSb heterostructures. With the successful growth of single and multiple layer heterostructures by different techniques, a wide range of material-related properties have been studied. At this time, the examination of optical properties in the multilayer and superlattice structures is being explored by photoluminescence and Raman scattering techniques. In parallel with these studies, various CdTe/InSb heterointerfacial regions are being examined by HREM imaging techniques in an attempt to isolate the existence of interfacial layers.

The potential for device applications has been established with the growth of multiple InSb-CdTe layered structures exhibiting high structural quality. The growth of $Cd_xMn_{1-x}Te$ in place of CdTe as a barrier layer to InSb may prove interesting, given that a small fraction of manganese should provide for an exact lattice matching between materials. The examination of transport properties in InSb epitaxial layers may be explored for the growth of InSb on InSb or CdTe substrates. One structure, having a great deal of technological importance, would be an MIS capacitor utilizing CdTe or $Cd_xMn_{1-x}Te$ as an insulator to InSb. In this way, C-V profiling could be used to further characterize the interfacial region of insulator on InSb. For the long term, examination of III-V/II-VI heterostructures, in general, would appear to be of great scientific interest given the possibility for useful device applications.

LIST OF REFERENCES

LIST OF REFERENCES

1. J. Tersoff, Phys. Rev. Lett. **56,** 2755 (1986).

2. K. J. Mackey, P. M. G. Allen, W. G. Herrenden-Harker and R. H. Williams, Surface Sci. **178,** 124 (1986).

3. R. G. van Welzenis and B. K. Ridley, Solid State Electron. **27,** 113 (1984).

4. Y-D. Zheng, Y. H. Chang, B. D. McCombe, R. F. C. Farrow, T. Temofonte, and F. A. Shirland, Appl. Phys. Lett. **49** (18), 1187 (1986).

5. Z. C. Feng, A. Mascarenhas, W. J. Choyke, R. F. C. Farrow, F. A. Shirland, and W. J. Takei, Appl. Phys. Lett. **47** (1) 24 (1985).

6. R. F. C. Farrow, G. R. Jones, G. M. Williams and I. M. Young, Appl. Phys. Lett. **39,** 954 (1981).

7. S. Wood, J. Greggy, Jr., R. F. C. Farrow, W. J. Takei, F. A. Shirland and A. J. Noreika, J. Appl. Phys. **55,** 4225 (1984).

8. G. M. Williams, C. R. Whitehouse, N. G. Chew, G. W. Blackmore and A. G. Cullis, J. Vac. Sci. Technol. B **3,** 704 (1985).

9. G. M. Williams, C. R. Whitehouse, T. Martin, N. G. Chew, A. G. Cullis, T. Ashley, D. E. Sykes, K. Mackey, and R. H. Williams J. Appl. Phys. **63,** (5) 1526 (1988).

10. K. Sugiyama, J. Crystal Growth **60,** 450 (1982).

11. L. A. Kolodziejski, R. L. Gunshor, N. Otsuka and A. V. Nurmikko, Mat. Res. Soc. Symp. **102,** 113 (1988).

12. R. L. Gunshor, L. A. Kolodziejski, M. R. Melloch, N. Otsuka, and A. V. Nurmikko, paper presented at the NATO Advanced Research Workshop on Wide Gap Low Dimensional II-VI's, Regensburg, West Germany, August 2-5, 1988.

13. T. D. Golding, M. Martinka, and J. H. Dinan, J. Appl. Phys. **64,** 1873 (1988).

14. Q-D. Qian, J. Qui, J. L. Glenn, Sungki O, R. L. Gunshor, L. A. Kolodziejski, M. Kobayashi, N. Otsuka, M. R. Melloch, J. A. Cooper Jr., M. Haggerott, T. Heyen, and A. V. Nurmikko. Procedings of the 5th International Conference on Molecular Beam Epitaxy. Saporo, August 1988, to appear in J. Crystal Growth.

15. J. L. Glenn Jr., Sungki O, L. A. Kolodziejski, R. L. Gunshor, M. Kobayashi, J. M. Gansalves, N. Otsuka, M. Haggerott, T. Heyen, and A. V. Nurmikko, to appear in J. Vac. Sci. Technol. (1989).

16. J. L. Glenn, Jr., Sungki O, R. L. Gunshor, L. A. Kolodziejski, M. Kobayashi, D. Li, N. Otsuka, M. Haggerott, N. Pelekanos, and A. V. Nurmikko, to appear in Appl. Phys. Lett. (1989).

17. G. M. Williams, C. R. Whitehouse, A. G, Cullis, N. G, Chew, and G. W. Blackmore, Appl. Phys. Lett. **53,** 1847 (1988).

18. A. J. Norieka, J. Greggi, Jr., W. J. Takei, and M. H. Francombe, J. Vac. Sci. Technol. A **1** (2), 558 (1983).

19. K. J. Mackey, D. R. Zahn, P. M. G. Allen, R. H. Williams, W. Richter, and R. S. Williams, J. Vac. Sci. Technol. B **5,** 1233 (1987).

20. K. Oe, S. Ando, and K. Sugiyama, Jpn. J. Appl. Phys. **19,** L417 (1980).

21. A. J. Noreika, M. H. Francombe, and C. E. C. Wood, J. Appl. Phys. **52,** 7416 (1981).

22. D. L. Rode, Phys. Rev. B **3,** 3287 (1971).

23. A. J. Bosch, R. G. van Welzenis, and O. F. Z. Schannen, J. Appl. Phys., **58,** 3434 (1985).

24. R. Dawson, private communication.

25. C. E. C. Wood, K. Singer, T. Ohashi, L. R. Dawson, and A. J. Noreika, J. Appl. Phys. **54** (5) 2732 (1983).

26. R. L. Anderson, Solid State Electron., **5,** 341 (1962).

27. R. F. Brebeck and A. J. Strauss, J. Phys. Chem. Solids., **25,** 1441 (1964).

28. R. F. C. Farrow, S. Wood, J. C. Greggi, Jr., W. J. Tahei, and F. A. Shirland, J. Vac Sci. Technol. B **3** (2) 681 (1985).

29. D.-W. Tu and A. Kahn, J. Vac. Sci. Technol. A **3** (3), 922 (1985).

30. InSb wafers were purchased from Cominco Electronic Materials Inc.

31. CdTe wafers were purchased from Galtech Semiconductors Inc.

32. J. H. Neave, P. Blood, and B. A. Joyce, Appl. Phys. Lett. **36** (4) 311 (1980).

33. M. Missous and K. E. Singer, Appl. Phys. Lett., **50** (11) 694 (1987).

34. E. H. C. Parker, ed. **The Technology and Physics of Molecular Beam Epitaxy,** Plenum Press: New York (1985).

35. Infrared pyrometer was aquirred from IRCON Inc. and operates at a detection wavelength of 2.0 - 2.6 μm.

36. CdTe source material purchased from II-VI Company Inc. was examined for total impurity concentration by Spark Source Mass Spectroscopy through Walters Chemical Consulting Inc.

37. A. Moouradian, and H. Y. Fan, Phys. Rev., **148** 873 (1966).

38. J. Pehek and H. Levinstein, Phys. Rev. **140,** A576 (1965).

39. J. D. Benson and C. J. Summers, J. Crystal Growth **86,** 354 (1988).

40. A. G. Cullis, N. G. Chew, and J. L. Hutchison, Ultramicroscopy **17,** 203 (1985).

41. Z. C. Feng, M. G. Burke, W. J. Choyke, Appl. Phys. Lett. **53,** (2) 128 (1988).

42. Y. R. Lee, A. K. Ramdas, L. A. Kolodziejski and R. L. Gunshor, to be published.

43. P. Heisinger, S. Suga, F. Willmann, W. Dreybrodt, Phys. Stat. sol. (b) **67,** 641 (1975).

44. N. Otsuka, private communication.

45. R. Venkatasubramanian, private communication.

46. T. Golding, private communication.

APPENDICES

APPENDIX A
FLUX CALIBRATION

A.1 Procedure for Flux Calibration

For the purpose of deriving a relationship between effusion cell temperature and molecular beam flux, at the sample location, a flux calibration procedure has been performed on each of the indium and antimony sources used in this work. The first phase of this procedure was to establish a theoretical flux-vs-temperature curve for each effusion cell by use of the ideal Knudsen cell equation (equation A1) [34].

$$J=(1.118x10^{22})\left\{\frac{pA}{l^2(MT)^{1/2}}\right\}(\cos\Theta)\text{molecules/cm}^2\text{sec} \qquad \text{(A1)}$$

In equation A1, p(Torr) is the vapor pressure in the cell for a material at temperature T(K) and with a molecular weight M(gms/mol). The equation applies for an effusion cell with an aperture of area A(cm^2) which is at a distance l(cm) from the substrate surface. The effusion source is directed towards the substrate at an angle "Θ" to the substrate surface normal. The molecular beam flux is therefore reduced at the substrate surface by a factor of cosΘ. The results obtained from calculating discrete flux-vs-temperature values from equation A1 were plotted on a semi-log graph. A typical flux-versus-temperature curve is shown, for a 60cc indium oven, in Figure A.1. To obtain actual flux values, a film of indium was deposited on a silicon substrate, with the substrate at room temperature (cold deposition). For the deposition, the silicon substrate was solvent degreased, rinsed in deionized water and etched in concentrated HF for 5 minutes to remove surface oxides. The wafer was then rinsed in deionized water and mounted, with indium, on a Mo sample holder. A small piece of Ni foil (approximately 1cm^2) was secured, with Ni wire, over a small central portion of the wafer to partially shield the

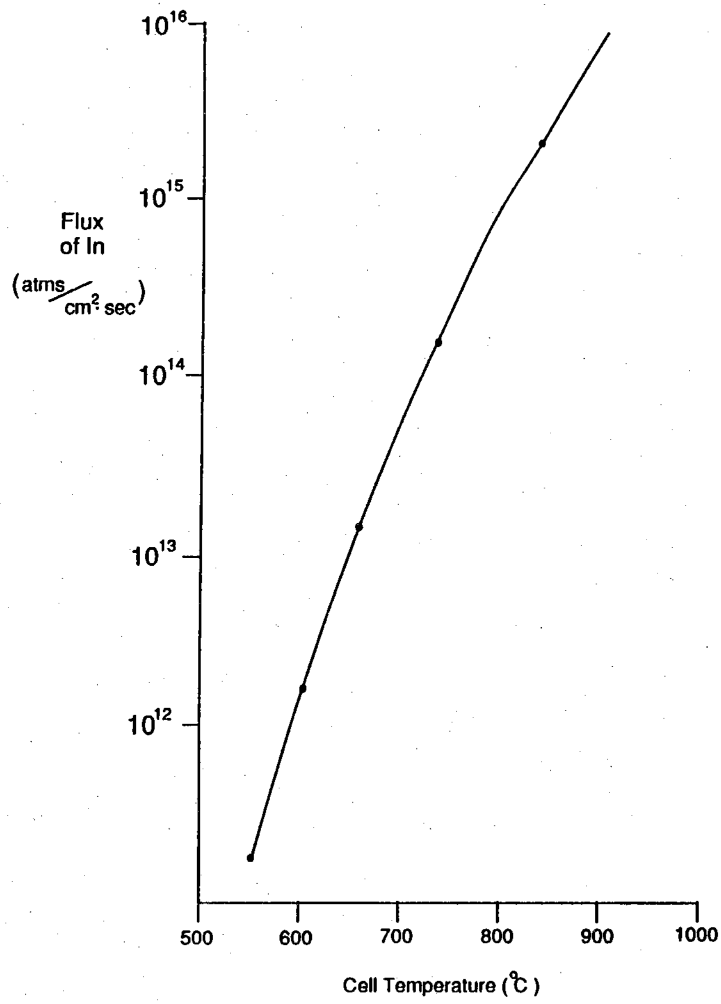

Figure A.1 Indium-flux versus cell-temperature for a 60cc crucible.

substrate from indium flux. After the cold deposition, the sample was removed from the block along with the Ni shield.

Using an alpha-step 200 surface profiler, a measure of indium film thickness was obtained by scanning the profiler stylus from the area where indium was deposited to the area which was shielded by the Ni foil (scanning over a step edge). Similar deposition procedures were then performed for the InSb, elemental antimony and antimony cracking cell ovens. Using standard values for the density and atomic weight of indium and antimony, the film thickness was correlated to a flux by use of equation A2.

$$J=(6.023x10^{23})\left\{\frac{\rho t}{\tau M}\right\}(\text{atoms/cm}^2\text{sec}) \qquad \text{(A2)}$$

In equation A2, ρ(gms/cm^3) is the mass density of the material in question, t(cm) is the cold deposition film thickness and τ(sec) is the time taken for deposition of the material. A list of the parameters used in solving equation A1 and equation A2 are given in Table A.1. The data gathered by cold deposition experiments was subsequently plotted beside the theoretical curve generated by use of equation A1. A new flux-versus-temperature curve was then generated by shifting the ideal curve (laterally) to pass through the experimental data point.

A.2 Results

Measurement of deposited film thickness was undoubtedly the largest source of error in determining experimental flux values. The error, in this case, arose from the observation that the deposited film surfaces were non-uniformly rough (in the surface profiler scans taken) making it somewhat difficult to determine the actual layer thickness. While the antimony depositions were seen to yield relatively flat surface profiler traces, the deposited indium surface was observed to be extremely rough. Determining the thickness of the deposited indium was therefore performed by averaging the thickness variations which were observed in the profiler scans taken.

Table A1 Parameters for calculating the indium and antimony flux for a 60cc crucible.

SYMBOL	DEFINITION	VALUE	ORIGIN
ρ (gms/cm^3)	density	7.31	indium
		6.691	antimony
M (gms/mol)	atomic weight	114.82	indium
		121.75	antimony
Θ ($^\circ$)	projection angle	24 $^\circ$	430 MBE
l (cm)	flux path length	20.23	430 MBE
A (cm^2)	aperture area	11.34	60cc oven

ACKNOWLEDGMENTS

Many people have made significant contributions to the work presented in this report. The authors would like to acknowledge the efforts of Dave Lubelski, Doug Menke Anant K. Ramdas, Michael R. Melloch, R. Venkatasubramanian, David L. Mathine, Du Li, J. M. Gonsalves, M. Haggerott, N. Pelekanos, and Yung-Rai R. Lee. Research support at Purdue was provided by SDIO/IST-Naval Research Laboratory Contract N00014-86-K2017, the Nation Science Foundation-MRG Grant DMR-8520866, and a joint AFOSR/ONR Research Instrumentation Grant N00014-86-G-0156.